

# The Optical Gravitational Lensing Experiment.

## Catalog of RR Lyrae Stars

### from the Small Magellanic Cloud\*

I. Soszynski<sup>1,2</sup>, A. Udalski<sup>1</sup>, M. Szymanski<sup>1</sup>,  
 M. Kubicki<sup>1</sup>, G. Pietrzynski<sup>1,3</sup>, P. Wozniak<sup>4</sup>,  
 K. Zebrun<sup>1</sup>, O. Szewczyk<sup>1</sup> and L. Wyrykowski<sup>1</sup>

<sup>1</sup> Warsaw University Observatory, Al. Ujazdowskie 4, 00-478 Warszawa, Poland  
 e-mail:

(soszynsk,udalski,msz,mk,pietrzyn,zebrun,szewczyk,wyrzykow)@astrouw.edu.pl

<sup>2</sup> Princeton University Observatory, Princeton, NJ 08544-1001 USA

<sup>3</sup> Universidad de Concepción, Departamento de Fisica, Casilla 160-C,  
 Concepción, Chile

<sup>4</sup> Los Alamos National Laboratory, MS-D436, Los Alamos, NM 87545 USA  
 e-mail: wozniak@lanl.gov

#### ABSTRACT

We present the catalog of RR Lyrae stars from 2.4 square degrees of central parts of the Small Magellanic Cloud (SMC). The photometric data were collected during four years of the OGLE-II microlensing survey. Photometry of each star was obtained using the Difference Image Analysis (DIA) method. The catalog contains 571 objects, including 458 RRab, 56 RRc variables, and 57 double mode RR Lyr stars (RRd). Additionally we attach a list of variables with periods between 0.18–0.26 days, which are probably δ Sct stars. Period, *BVI* photometry, astrometry, amplitude, and parameters of the Fourier decomposition of the *I*-band light curve are provided for each object. We also present the Petersen diagram for double mode pulsators.

We found that the SMC RR Lyr stars are fairly uniformly distributed over the studied area, with no clear correlation to any location. The most preferred periods for RRab and RRc stars are 0.589 and 0.357 days, respectively. We noticed significant excess of stars with periods of about 0.29 days, which might be second-overtone RR Lyr stars (RRe). The mean extinction free magnitudes derived for RRab stars are 18.97, 19.45 and 19.73 mag for the *I*, *V* and *B*-band, respectively.

All presented data, including individual *BVI* observations, are available from the OGLE INTERNET archive.

---

\*Based on observations obtained with the 1.3 m Warsaw telescope at the Las Campanas Observatory of the Carnegie Institution of Washington.

## 1. Introduction

The Magellanic Clouds provide an ideal opportunity to study in detail the structure and evolution of stars. Rich populations of stars approximately at the same, relatively small distance with small interstellar reddening make the Large and Small Magellanic Clouds very important targets for observing surveys.

RR Lyr stars were first discovered in the SMC near the cluster NGC121 by Thackeray (1951). The stars were more than a magnitude fainter than expected, what was a crucial confirmation of the major revision of the extragalactic distance scale proposed by Baade (1952). The first systematic search for field RR Lyr variables in the SMC was conducted by Graham (1975). During that survey 76 RR Lyr stars were discovered in a  $1^\circ \times 1.3^\circ$  outlying field centered on the cluster NGC121. Smith *et al.* (1992) used *B*-band photographic photometry of a field in the northeast arm of the SMC to identify additional 22 probable RR Lyr variables. The same outlying region of the SMC was observed by Sharpee *et al.* (2002). They presented *V*-band and *B*-band CCD photometry of a few RR Lyr stars.

Walker (1989) surveyed five SMC clusters for RR Lyr stars. Four already known RR Lyr variables in the NGC121 were rediscovered, but no such stars were found in the other clusters. Because the age of NGC121 was estimated to be  $12 \pm 2$  Gyr (Stryker *et al.* 1985), and Lindsay 1, the next oldest SMC cluster,  $10 \pm 2$  Gyr (Olszewski *et al.* 1987), Walker concluded that the minimum age of RR Lyr stars is about 11 Gyr.

In 1990s the number of known variable stars in the Magellanic Clouds dramatically increased, when the large microlensing searches began regular photometric monitoring of both galaxies (*e.g.*, MACHO – Alcock *et al.* 1993, EROS – Aubourg *et al.* 1993). Natural by-product of the microlensing surveys are huge databases with precise photometry of millions of stars.

The SMC was also included to the list of targets of the second phase of the Optical Gravitational Lensing Experiment (OGLE-II; Udalski, Kubiak and Szymański 1997). About 2.4 square degrees of central part of the SMC were observed each night during the observing seasons 1997–2000. Photometry was obtained with the *BVI* filters, closely resembling the standard system.

The OGLE-II survey has yielded a particularly rich harvest of variable stars from the SMC. In the previous papers we presented the catalog of eclipsing binary stars (Udalski *et al.* 1998b), the catalog of Cepheids from the SMC (Udalski *et al.* 1999), and general catalog of variable stars detected in the Magellanic Clouds (Żebruń *et al.* 2001). In addition *BVI* maps of the SMC were released providing precise photometry and astrometry of about 2.2 million stars (Udalski *et al.* 1998a).

In this paper we present a sample of 571 RR Lyr stars and several other pulsating objects, likely  $\delta$  Sct stars, detected in the OGLE-II fields in the SMC. The stars were selected from the reprocessed OGLE-II photometry based on the Difference Image Analysis (DIA) technique – Woźniak’s (2000) implementation of Alard and Lupton (1998) and Alard (2000) optimal Point Spread Function

matching algorithm.

Similarly to the previous catalogs, all data presented in this paper, including individual observations, are available to the astronomical community from the OGLE INTERNET archive.

## 2. Observations and Data Reductions

Observations presented in this paper were collected during the second phase of the OGLE microlensing search with the 1.3-m Warsaw telescope at Las Campanas Observatory, Chile. The observatory is operated by the Carnegie Institution of Washington. The telescope was equipped with the “first generation” camera with a SITe  $2048 \times 2048$  CCD detector working in drift-scan mode. The pixel size was  $24 \mu\text{m}$  giving the  $0.417 \text{ arcsec/pixel}$  scale. Observations of the SMC were performed in the “slow” reading mode of the CCD detector with the gain  $3.8 \text{ e}^-/\text{ADU}$  and readout noise of about  $5.4 \text{ e}^-$ . Details of the instrumentation setup can be found in Udalski, Kubiak and Szymański (1997).

Observations of the SMC were collected between June 26, 1997 and November 25, 2000. Eleven driftscan fields (SMC\_SC1–SMC\_SC11) covering about 2.4 square degrees of central parts of the SMC were observed. The majority of frames were taken in the  $I$  photometric band (about 280–340 epochs depending on the field). Other images were collected through the  $V$ -band (typically about 30 epochs) and  $B$ -band (about 20 epochs) filters. The effective exposure time lasted 125, 174 and 237 seconds for the  $I$ ,  $V$  and  $B$ -band, respectively. The median seeing was about  $1.^{\prime\prime}3$  for our dataset.

The  $I$ -band photometry was obtained using Difference Images Analysis (DIA) – image subtraction algorithm developed by Alard and Lupton (1998) and Alard (2000), and implemented by Woźniak (2000). We introduced several modifications compared to the DIA techniques employed in a catalog of variable stars in the Magellanic Clouds (Żebruń *et al.* 2001). For instance, we performed the DIA photometry for each star found in the reference image instead of the variable objects only. Further details of the DIA analysis and calibration of photometry may be found in the papers by Woźniak (2000) and by Żebruń, Soszyński and Woźniak (2001).

The frames in the  $V$  and  $B$  bands were analyzed using the DoPHOT photometry program (Schechter, Saha and Mateo 1993). Transformation of the instrumental photometry to the standard system is described by Udalski *et al.* (1998a).

Equatorial coordinates of all stars were calculated in the identical manner as described in Udalski *et al.* (1998a). The internal accuracy of the determined equatorial coordinates, as measured in the overlapping regions of neighboring fields, is about  $0.^{\prime\prime}15$ – $0.^{\prime\prime}20$  with possible systematic errors of the DSS coordinate system up to  $0.^{\prime\prime}7$ .

Fig. 1 presents the picture of the SMC from Digitized Sky Survey CD-ROMs with contours of the OGLE-II fields. Positions of RR Lyr stars are marked with black dots. One can easily notice that the surface density of RR Lyr variables is

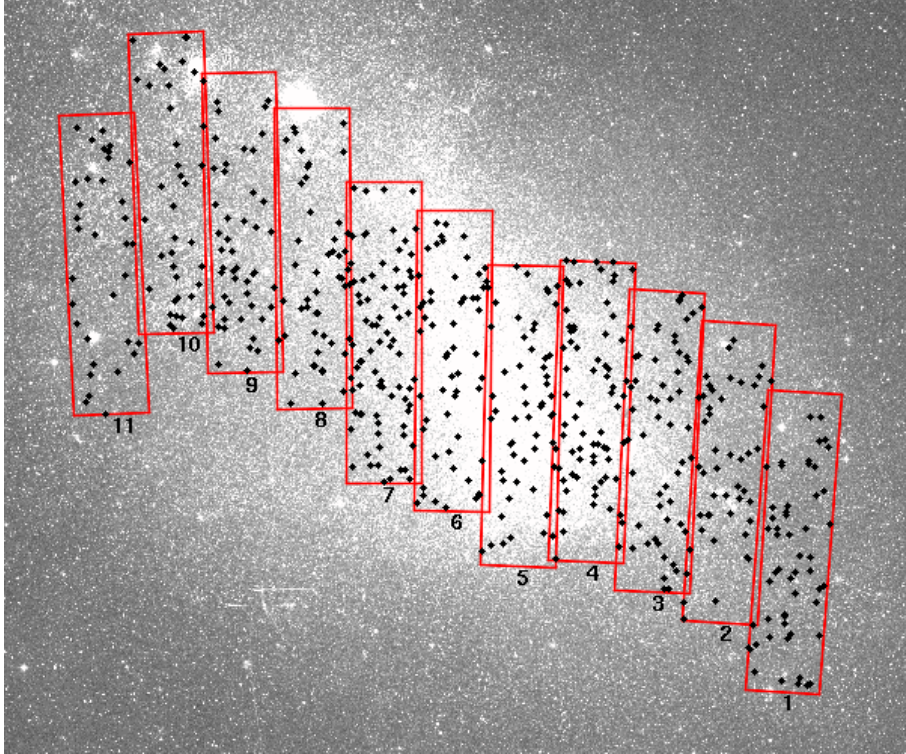


Fig. 1. OGLE-II fields in the SMC. Dots indicate positions of RR Lyr stars from the Catalog. North is up and East to the left in this Digitized Sky Survey image of the SMC.

very uniform within the galaxy. This confirms the results of Graham (1975) and Smith *et al.* (1992) who noticed that RR Lyr stars are not strongly concentrated toward either the bar or the center of the SMC.

### 3. Interstellar Reddening

Determination of the interstellar reddening to the SMC fields was performed by Udalski *et al.* (1999). In short, they used red clump stars for mapping the fluctuations of mean reddening in OGLE fields, treating their mean *I*-band magnitude as the reference brightness. Since reddening in the SMC is smaller and more homogeneous than in the LMC, it was determined only in 11 lines-of-sight – one per OGLE field. The zero point of the reddening map was derived on the basis of previous determinations toward two stars clusters: NGC416 and NGC330.

The final  $E(B-V)$  reddening in the SMC is listed in Table 1. The error of the map is equal to  $\pm 0.02$  mag. Similar values of reddening were estimated by Sharpee *et al.* (2002) for a field in the northeast arm of the SMC located close

T a b l e 1  
 $E(B-V)$  reddening in the SMC fields

Field	$E(B-V)$
SMC_SC1	0.070
SMC_SC2	0.078
SMC_SC3	0.089
SMC_SC4	0.094
SMC_SC5	0.101
SMC_SC6	0.094
SMC_SC7	0.097
SMC_SC8	0.100
SMC_SC9	0.076
SMC_SC10	0.079
SMC_SC11	0.084

to the OGLE fields SMC\_SC10 and SMC\_SC11. Interstellar extinction in the  $BVI$  bands can be calculated using the standard extinction curve coefficients (e.g., Schlegel *et al.* 1998):

$$A_B = 4.32 \cdot E(B-V), \quad A_V = 3.24 \cdot E(B-V), \quad A_I = 1.96 \cdot E(B-V)$$

#### 4. Selection of RR Lyr Stars

Selection of RR Lyr stars was performed in two stages. First, preliminary search for variable stars was performed using the regular OGLE-II PSF (DoPHOT) photometry. The mean  $I$ -band magnitude of objects was limited to  $I < 20$  mag. The minimal number of individual measurements was set to 50. Candidates for variable stars were selected based on comparison of the standard deviation of photometry with typical standard deviation for stars with similar brightness. Light curves of selected candidates were searched for periodicity using the AoV algorithm (Schwarzenberg-Czerny 1989). Light curves of all objects revealing statistically significant periodic signal were then visually inspected. Candidates for RR Lyr stars were extracted on the basis of light curve shapes and magnitudes of the stars.

The second, final search for RR Lyr variables was performed with the DIA photometry of all stars detected in the reference images. The quality of DIA photometry is improved by a factor of at least two, compared to the DoPHOT photometry (Woźniak 2000), what enabled us to increase considerably the completeness of the catalog.

We examined with the AoV period search technique the DIA photometry of objects with the mean magnitude  $18.4 < I < 19.4$  and standard deviation at least 0.02 mag larger than typical standard deviation for non-variable stars of similar brightness. Additionally we checked stars with the  $V$ -band magnitude between 18.9 and 20.0 and the standard deviation of  $V$ -band photometry 0.05 mag larger

than typical. New candidates for RR Lyr stars were selected from a sample of stars with periods smaller than 1 day based on visual inspection of their light curves and location in the color-magnitude diagram (CMD).

The second stage of variability search increased the number of candidates for RR Lyr stars by about 30%. In total 571 candidates for RR Lyr stars were identified. Several objects with colors outside the range  $0.2 < V - I < 0.8$  and objects with no color information but with evident RR Lyr-type light curves were also included to this sample. They can be highly reddened or blended stars.

## 5. Classification

We divided all objects into four groups: fundamental mode RR Lyr stars (RRab), first overtone (RRc), double mode RR Lyr stars (RRd) and other variable stars, which, in the majority of cases, are probably  $\delta$  Sct stars.

Selection of RRab-type stars from our sample was not difficult, because these variables form well separated groups in various diagrams. We decided to use period-amplitude diagram to classify fundamental-mode pulsators, because periods and amplitudes are the observables that are measured with the highest precision.

There were more problems with separation of the first overtone RR Lyr stars and short-period variable stars. Both groups of objects in our sample have similar luminosities, amplitudes and shapes of light curve. Additionally, the range of periods of  $\delta$  Sct stars overlaps with the range of periods of RRc variables.

The models of Bono *et al.* (1997) predict that the first-overtone RR Lyr stars with the shortest periods should have the lowest amplitudes. Indeed, in the period-amplitude diagrams (Fig. 4) one can notice a minimum of IV-band amplitudes near the period of about 0.26 days. Therefore, we decided to mark as the first overtone RR Lyr candidates with periods larger than 0.26 days. Objects with shorter periods were classified as  $\delta$  Sct stars. However, we stress that it is possible that some of the RRc variables on our list are  $\delta$  Sct or other types of variable stars, and *vice versa*. It is also possible that some second-harmonic RR Lyr stars (RRe) can be included in the short period group. Further observations, especially in the Strömgren *uvby* filters, could provide additional information for final classification.

We used two methods to search for multi-periodic variable stars. First, we fitted a fourth order Fourier series to each folded light curve from our sample and subtracted fitted function from the observational data. Then, the residuals were searched for periodic signal and, if detected, such a candidate was marked for visual inspection.

Second search for double-mode RR Lyr stars was performed using the CLEAN algorithm of period determination (Roberts, Lehár and Dreher 1987). All RR Lyr candidates from our list were subject to the CLEAN period analysis. In further analysis we selected objects for which the ratio of the highest peak in

the power spectrum and one of the next four strongest peaks was close to 0.745.

Final list of the double-mode variable stars presented in this paper was obtained after careful visual inspection of power spectra and folded light curves of candidates. We identified 57 RRd stars, 2 double mode  $\delta$  Sct stars and several dozen stars with two closely spaced frequencies, that are probably members of a new class of multi-periodic RR Lyr stars described by Olech *et al.* (1999). About 10% in both, RRab and RRc groups, exhibited secondary periodicity very close to the primary pulsation frequency, with period ratios in the range 0.98–1.02. This frequency pattern cannot be explained by a superposition of radial pulsations and is therefore believed to be related to non-radial modes. Non-radial oscillations have also been detected in some RR Lyr stars in the Galactic bulge by Moskalik (2000) and in the LMC by Kovács *et al.* (2000). Theoretical models of these stars have been proposed by Dziembowski and Cassisi (1999).

## 6. Catalog of RR Lyr Stars

### 6.1 Single-Mode RR Lyr Stars

458 RRab and 56 RRc variable stars passed our selection criteria. They are listed in Tables 2 and 3. First two columns of both tables contain the star identification: field\_name star\_ID. The star\_IDs are simultaneously equatorial coordinates, RA and DEC (J2000), of the objects. In the next columns period in days and moment of the zero phase corresponding to maximum light are given. Finally, last columns show intensity mean *IVB* photometry.

More parameters (period errors, Fourier parameters of the light curve decomposition, *IVB*-band amplitudes) are available in the electronic form from the OGLE INTERNET archive:

```
http://www.astroww.edu.pl/~ogle/
ftp://sirius.astroww.edu.pl/ogle/ogle2/var\_stars/smc/rrlyr/
```

or its US mirror

```
http://bulge.princeton.edu/~ogle/
ftp://bulge.princeton.edu/ogle/ogle2/var\_stars/smc/rrlyr/
```

Also individual *BVI* observations of all objects and finding charts are included.

Tables 2 and 3 contain together 536 entries but only 514 objects, because 22 stars were detected twice – in the overlapping regions of adjacent fields. We decided not to remove twice-detected RR Lyr stars from the final list, because their measurements are independent in both fields and can be used for testing quality of data and completeness of the sample. In Table 6 we provide cross-reference list to identify stars in the overlapping regions.

In Fig. 2 we present *I*-band light curves of a few typical RRab, RRc stars and one RRd star. All the diagrams have the same magnitude range to compare the amplitudes and brightness of the stars. The light curves are arranged according to the periods.

T a b l e 2  
ab-type RR Lyrae stars from the SMC

Field	Star ID	$P$ [days]	$T_0$ [HJD]	$I$ [mag]	$V$ [mag]	$B$ [mag]
SMC_SC1	OGLE003707.89–735613.9	0.628518	2450450.08631	18.91	19.46	19.80
SMC_SC1	OGLE003642.77–735612.1	0.525673	2450450.01915	19.25	19.79	–
SMC_SC1	OGLE003752.40–735555.9	0.577047	2450450.15096	18.99	19.60	19.82
SMC_SC1	OGLE003634.14–735553.1	0.633026	2450450.33529	19.12	19.76	20.09
SMC_SC1	OGLE003707.32–735455.8	0.562787	2450450.46047	19.17	19.66	20.00
SMC_SC1	OGLE003925.15–735015.8	0.689856	2450450.07815	18.61	19.30	19.78
SMC_SC1	OGLE003909.14–734921.4	0.564473	2450450.45890	18.70	19.23	19.55
SMC_SC1	OGLE003836.02–734750.2	0.583830	2450450.12202	19.19	19.80	20.12
SMC_SC1	OGLE003623.02–734651.0	0.565954	2450450.30161	19.01	19.51	19.83
SMC_SC1	OGLE003920.43–734540.7	0.600827	2450450.56287	19.07	19.69	19.96
SMC_SC1	OGLE003756.32–734508.8	0.588990	2450450.32308	19.12	19.75	20.09
SMC_SC1	OGLE003841.21–734422.9	0.410569	2450450.35916	19.54	20.02	20.22
SMC_SC1	OGLE003758.84–734339.5	0.523207	2450450.04769	19.11	19.60	19.93
SMC_SC1	OGLE003757.71–734326.9	0.583903	2450450.37033	18.70	19.24	19.55
SMC_SC1	OGLE003737.63–733914.6	0.588109	2450450.45983	19.18	19.70	20.07
SMC_SC1	OGLE003633.22–733800.8	0.630791	2450450.32372	19.02	19.57	19.93
SMC_SC1	OGLE003620.57–733724.0	0.639572	2450450.05727	19.12	19.70	20.20
SMC_SC1	OGLE003847.37–733715.8	0.698386	2450450.36581	19.05	19.68	20.08
SMC_SC1	OGLE003750.29–733633.9	0.575954	2450450.30285	18.93	19.46	19.71
SMC_SC1	OGLE003881.01–733539.7	0.613462	2450450.36119	19.14	19.71	20.07
SMC_SC1	OGLE003739.99–733513.5	0.667574	2450450.22469	19.11	19.75	20.14
SMC_SC1	OGLE003824.91–733500.5	0.602657	2450450.33238	19.07	19.64	19.92
SMC_SC1	OGLE003731.46–733210.8	0.687784	2450450.57565	18.84	19.44	19.81
SMC_SC1	OGLE003834.63–732829.9	0.608249	2450450.33384	18.83	19.32	19.61
SMC_SC1	OGLE003901.88–732727.5	0.582833	2450450.37265	18.73	19.39	19.32
SMC_SC1	OGLE003839.07–732726.0	0.547269	2450450.31495	19.19	19.70	20.03
SMC_SC1	OGLE003723.52–732700.6	0.522510	2450450.02864	19.21	19.70	20.07
SMC_SC1	OGLE003851.89–732530.1	0.593166	2450450.04659	19.18	19.68	19.99
SMC_SC1	OGLE003816.46–732449.2	0.427897	2450450.16153	19.45	19.77	20.04
SMC_SC1	OGLE003815.86–732403.7	0.588187	2450450.29876	19.16	19.97	20.00
SMC_SC1	OGLE003814.29–732257.8	0.485913	2450450.12678	19.14	19.63	19.94
SMC_SC1	OGLE003700.85–732038.6	0.496091	2450450.20237	19.39	19.90	20.17
SMC_SC1	OGLE003640.43–731943.1	0.642239	2450450.15996	18.97	19.52	19.90
SMC_SC1	OGLE003915.76–731555.1	0.517790	2450450.04688	19.13	19.64	19.91
SMC_SC1	OGLE003836.32–731526.8	0.636549	2450450.25708	19.13	19.82	20.18
SMC_SC1	OGLE003711.49–731513.2	0.657652	2450450.45133	18.99	19.63	–
SMC_SC1	OGLE003727.78–731454.9	0.412698	2450450.33535	19.51	20.02	20.29
SMC_SC1	OGLE003726.21–731420.0	0.519471	2450450.31104	19.13	19.59	19.90
SMC_SC1	OGLE003641.77–731120.1	0.598166	2450450.51871	19.04	19.57	–
SMC_SC1	OGLE003704.40–731023.2	0.651941	2450450.55886	18.78	19.31	19.72
SMC_SC1	OGLE003648.60–731003.0	0.554478	2450450.06475	19.30	19.95	–
SMC_SC2	OGLE004231.36–734227.2	0.551124	2450450.31254	19.13	19.72	–
SMC_SC2	OGLE004227.44–733655.1	0.658287	2450450.65074	19.03	19.64	20.04
SMC_SC2	OGLE003951.38–733307.7	0.520450	2450450.20499	19.16	19.64	19.89
SMC_SC2	OGLE004123.87–733024.5	0.633188	2450450.06167	18.78	19.35	–
SMC_SC2	OGLE003959.69–732855.3	0.639105	2450450.07035	19.20	19.81	20.23
SMC_SC2	OGLE004156.67–732831.6	0.568383	2450450.03657	18.90	19.43	19.74
SMC_SC2	OGLE003950.33–732627.0	0.635539	2450450.13159	19.08	19.72	20.11
SMC_SC2	OGLE004143.00–732553.5	0.570230	2450450.51291	19.05	19.48	19.83
SMC_SC2	OGLE004138.10–732540.6	0.555241	2450450.28273	19.27	19.79	20.10
SMC_SC2	OGLE004043.07–732509.1	0.649512	2450450.21117	19.00	19.62	20.17
SMC_SC2	OGLE003953.93–732246.5	0.604904	2450450.04027	19.01	19.53	19.90
SMC_SC2	OGLE004022.62–732222.4	0.580435	2450450.26546	19.23	19.79	20.13
SMC_SC2	OGLE004129.39–732202.3	0.629913	2450450.18934	19.24	19.86	20.04
SMC_SC2	OGLE004059.14–732155.8	0.749157	2450450.38856	19.15	19.76	20.23
SMC_SC2	OGLE004010.03–732044.6	0.583876	2450450.38355	19.44	20.05	20.38
SMC_SC2	OGLE004027.63–731954.9	0.595305	2450450.26668	19.44	20.02	20.44
SMC_SC2	OGLE004202.17–731758.8	0.572903	2450450.15389	19.04	19.60	20.00
SMC_SC2	OGLE004025.49–731452.5	0.605694	2450450.58069	19.25	19.83	20.28
SMC_SC2	OGLE004131.78–731328.5	0.604973	2450450.23258	19.02	19.59	–
SMC_SC2	OGLE003943.19–731245.9	0.593981	2450450.28635	18.91	19.32	19.56
SMC_SC2	OGLE004204.03–730813.5	0.636453	2450450.29674	19.17	19.75	20.24
SMC_SC2	OGLE004156.46–730641.7	0.586298	2450450.17198	19.13	–	–
SMC_SC2	OGLE004154.36–730539.3	0.524564	2450450.23252	19.27	19.80	20.18
SMC_SC2	OGLE004126.84–730355.2	0.705041	2450450.68756	18.89	19.58	20.11
SMC_SC2	OGLE004225.29–730349.8	0.699868	2450450.24522	18.88	19.34	19.77
SMC_SC2	OGLE004211.68–730329.2	0.632047	2450450.21854	19.34	20.04	20.54
SMC_SC2	OGLE004150.76–730220.5	0.578257	2450450.49694	19.19	19.88	20.34

Table 2

Continued

Field	Star ID	$P$ [days]	$T_0$ [HJD]	$I$ [mag]	$V$ [mag]	$B$ [mag]
SMC_SC2	OGLE003922.76–725950.6	0.544786	2450450.13952	19.21	19.85	–
SMC_SC2	OGLE004206.40–725949.0	0.608147	2450450.04027	19.19	19.86	20.29
SMC_SC2	OGLE004106.44–725948.4	0.510413	2450450.35386	19.28	19.83	20.21
SMC_SC2	OGLE003952.24–725901.7	0.591274	2450450.33622	19.12	19.67	19.99
SMC_SC2	OGLE003947.05–725700.1	0.554868	2450450.28534	19.06	19.56	19.90
SMC_SC2	OGLE004105.74–725238.1	0.539650	2450450.52923	18.91	19.38	19.66
SMC_SC3	OGLE004324.97–734011.6	0.585206	2450450.01341	19.08	–	20.01
SMC_SC3	OGLE004312.60–734000.8	0.508109	2450450.48203	19.24	19.86	20.08
SMC_SC3	OGLE004326.58–733809.2	0.583202	2450450.41598	19.20	19.80	20.36
SMC_SC3	OGLE004227.44–733655.1	0.658282	2450450.00702	19.05	19.64	20.05
SMC_SC3	OGLE004258.04–733642.7	0.636162	2450450.18009	18.91	19.41	19.83
SMC_SC3	OGLE004306.71–733527.9	0.466095	2450450.33967	19.60	19.98	20.32
SMC_SC3	OGLE004454.78–733241.3	0.567085	2450450.02131	19.14	19.72	20.08
SMC_SC3	OGLE004533.91–733240.3	0.594071	2450450.12923	19.37	19.87	20.16
SMC_SC3	OGLE004416.71–733148.7	0.674706	2450450.14972	19.24	19.94	20.40
SMC_SC3	OGLE004350.56–733141.1	0.588695	2450450.18045	19.06	19.66	20.03
SMC_SC3	OGLE004356.46–733045.4	0.535740	2450450.51319	19.28	19.88	20.30
SMC_SC3	OGLE004238.25–732911.4	0.578983	2450450.18109	19.28	19.90	20.39
SMC_SC3	OGLE004526.76–732801.7	0.613725	2450450.55600	19.20	19.92	20.31
SMC_SC3	OGLE004329.74–732705.8	0.564446	2450450.42257	19.20	19.72	20.13
SMC_SC3	OGLE004531.73–732634.2	0.507230	2450450.35151	19.41	19.92	20.23
SMC_SC3	OGLE004323.58–732338.5	0.631343	2450450.27193	19.06	19.63	20.00
SMC_SC3	OGLE004351.26–732225.9	0.652652	2450450.15028	19.33	20.05	–
SMC_SC3	OGLE004506.65–731845.6	0.667459	2450450.17054	19.28	20.12	20.59
SMC_SC3	OGLE004307.06–731808.6	0.581089	2450450.30603	19.14	19.65	19.80
SMC_SC3	OGLE004256.85–731612.8	0.516150	2450450.04373	19.59	20.16	20.55
SMC_SC3	OGLE004236.24–731512.1	0.593325	2450450.16000	19.15	19.83	20.35
SMC_SC3	OGLE004533.00–731255.1	0.601841	2450450.23558	18.86	19.38	–
SMC_SC3	OGLE004520.13–731233.5	0.579379	2450450.55955	19.52	20.32	20.75
SMC_SC3	OGLE004441.67–731126.2	0.760147	2450450.08199	18.94	19.57	19.98
SMC_SC3	OGLE004336.02–730919.6	0.613051	2450450.34229	19.08	19.66	19.99
SMC_SC3	OGLE004405.30–730800.8	0.559465	2450450.00829	19.54	19.98	20.12
SMC_SC3	OGLE004514.95–730638.7	0.619373	2450450.53815	18.78	19.55	–
SMC_SC3	OGLE004414.01–730449.8	0.474392	2450450.19235	19.36	19.89	20.32
SMC_SC3	OGLE004339.08–730426.5	0.588119	2450450.05648	19.17	19.69	20.05
SMC_SC3	OGLE004429.26–730421.4	0.520797	2450450.22782	18.69	19.10	19.53
SMC_SC3	OGLE004225.29–730349.8	0.699864	2450450.26169	18.82	–	–
SMC_SC3	OGLE004315.39–730300.3	0.624452	2450450.40185	19.09	19.65	20.15
SMC_SC3	OGLE004520.12–730224.8	0.659571	2450450.59086	19.26	20.03	20.52
SMC_SC3	OGLE004508.81–730126.7	0.700450	2450450.61532	19.02	19.49	19.76
SMC_SC3	OGLE004533.33–730120.2	0.572240	2450450.37587	18.99	–	–
SMC_SC3	OGLE004422.52–725710.3	0.656097	2450450.60125	19.07	19.69	20.08
SMC_SC3	OGLE004255.30–725707.7	0.590113	2450450.31280	19.18	19.74	20.09
SMC_SC3	OGLE004512.96–725645.9	0.552929	2450450.21355	19.29	19.83	20.23
SMC_SC3	OGLE004300.35–725626.0	0.543195	2450450.14120	18.91	19.36	19.64
SMC_SC3	OGLE004504.31–725623.9	0.567931	2450450.21802	19.08	19.62	19.92
SMC_SC3	OGLE004319.78–725523.9	0.589635	2450450.04537	19.04	19.57	19.95
SMC_SC3	OGLE004333.99–725339.4	0.616317	2450450.37327	19.19	19.82	20.20
SMC_SC3	OGLE004335.00–725231.3	0.586273	2450450.07666	19.27	19.80	20.20
SMC_SC3	OGLE004422.31–725127.9	0.645223	2450450.38919	19.10	19.77	20.24
SMC_SC3	OGLE004528.73–725109.7	0.656902	2450450.10323	19.06	19.71	20.15
SMC_SC3	OGLE004420.93–725034.4	0.616291	2450450.60864	19.18	19.81	20.23
SMC_SC3	OGLE004307.78–724922.1	0.585893	2450450.15964	19.20	19.74	20.17
SMC_SC3	OGLE004326.82–724559.3	0.567412	2450450.16543	19.22	19.77	20.25
SMC_SC3	OGLE004322.93–724447.5	0.648591	2450450.31631	18.86	19.45	19.84
SMC_SC4	OGLE004819.70–733521.5	0.596133	2450450.46771	19.28	–	–
SMC_SC4	OGLE004533.91–733240.3	0.594074	2450450.12299	19.35	19.75	19.89
SMC_SC4	OGLE004827.91–733108.7	0.637821	2450450.38748	18.98	19.57	19.99
SMC_SC4	OGLE004801.59–733021.5	0.399572	2450450.14594	19.49	19.91	20.21
SMC_SC4	OGLE004526.76–732801.7	0.613714	2450450.56070	19.23	19.87	–
SMC_SC4	OGLE004531.73–732634.2	0.507225	2450450.37273	19.46	19.88	20.30
SMC_SC4	OGLE004802.63–732627.0	0.610070	2450450.29492	18.96	19.56	19.92
SMC_SC4	OGLE004816.17–732618.9	0.599649	2450450.57126	19.29	20.14	20.38
SMC_SC4	OGLE004601.00–732535.3	0.588723	2450450.17922	18.96	19.50	19.82
SMC_SC4	OGLE004644.13–732500.7	0.622674	2450450.45496	18.25	18.42	18.51
SMC_SC4	OGLE004642.76–732311.2	0.619927	2450450.18659	18.97	19.80	20.16
SMC_SC4	OGLE004758.98–732241.3	0.449794	2450450.18042	19.80	20.46	20.91
SMC_SC4	OGLE004644.71–732140.8	0.574656	2450450.46645	19.11	19.51	19.70

Table 2

Continued

Field	Star ID	$P$ [days]	$T_0$ [HJD]	$I$ [mag]	$V$ [mag]	$B$ [mag]
SMC_SC4	OGLE004626.35–732039.2	0.613248	2450450.25379	19.39	20.18	20.74
SMC_SC4	OGLE004805.65–732033.9	0.523798	2450450.36642	19.24	19.63	19.93
SMC_SC4	OGLE004733.11–732004.3	0.592249	2450450.04479	19.30	20.02	20.55
SMC_SC4	OGLE004733.05–731955.4	0.656125	2450450.57332	19.29	19.92	20.16
SMC_SC4	OGLE004548.41–731955.3	0.695294	2450450.29419	19.36	19.51	19.98
SMC_SC4	OGLE004744.69–731919.1	0.598960	2450450.46312	19.12	19.71	20.18
SMC_SC4	OGLE004817.88–731815.2	0.558981	2450450.22373	19.03	19.61	19.91
SMC_SC4	OGLE004833.02–731700.0	0.535606	2450450.11273	19.39	20.00	20.48
SMC_SC4	OGLE004650.36–731652.2	0.630375	2450450.32362	19.00	19.60	20.00
SMC_SC4	OGLE004726.08–731632.0	0.563371	2450450.25654	19.05	20.02	–
SMC_SC4	OGLE004611.69–731625.0	0.554438	2450450.33012	19.39	20.06	20.55
SMC_SC4	OGLE004649.00–731544.5	0.665961	2450450.59371	18.98	19.59	19.89
SMC_SC4	OGLE004828.10–731442.2	0.586266	2450450.58390	18.74	19.28	19.59
SMC_SC4	OGLE004724.96–731427.2	0.614266	2450450.06254	18.95	19.54	19.95
SMC_SC4	OGLE004623.27–731356.1	0.584151	2450450.53290	19.32	19.89	20.18
SMC_SC4	OGLE004651.52–731333.7	0.487166	2450450.27109	19.79	20.36	20.79
SMC_SC4	OGLE004835.73–731330.1	0.584923	2450450.34526	19.21	19.96	–
SMC_SC4	OGLE004639.18–731324.7	0.424320	2450450.06714	19.60	20.04	20.34
SMC_SC4	OGLE004533.00–731255.1	0.601843	2450450.23359	18.88	19.41	19.80
SMC_SC4	OGLE004809.48–731209.0	0.606119	2450450.18750	19.39	19.78	20.21
SMC_SC4	OGLE004721.26–731135.5	0.462014	2450450.10985	19.46	19.97	20.84
SMC_SC4	OGLE004632.60–731109.4	0.685350	2450450.05829	19.02	19.64	20.04
SMC_SC4	OGLE004739.98–730843.0	0.590461	2450450.09431	18.89	19.29	19.63
SMC_SC4	OGLE004551.52–730620.0	0.618171	2450450.42983	19.07	19.67	20.14
SMC_SC4	OGLE004732.54–730610.3	0.471967	2450450.16210	19.73	20.56	–
SMC_SC4	OGLE004805.01–730426.6	0.545770	2450450.20954	19.33	19.88	20.27
SMC_SC4	OGLE004539.62–730422.2	0.605842	2450450.32578	19.32	19.86	20.66
SMC_SC4	OGLE004610.66–730355.6	0.611444	2450450.55907	19.23	–	–
SMC_SC4	OGLE004607.56–730236.0	0.657592	2450450.14296	18.86	19.42	19.73
SMC_SC4	OGLE004533.33–730120.2	0.572237	2450450.38078	19.04	19.50	19.83
SMC_SC4	OGLE004807.67–725937.8	0.626137	2450450.56625	18.37	19.10	19.59
SMC_SC4	OGLE004659.82–725937.7	0.651938	2450450.53632	18.95	19.82	19.67
SMC_SC4	OGLE004619.25–725914.3	0.587185	2450450.46039	19.25	19.82	20.30
SMC_SC4	OGLE004629.89–725841.9	0.563436	2450450.47365	19.44	20.14	20.56
SMC_SC4	OGLE004649.36–725742.5	0.635306	2450450.58726	18.95	19.47	19.78
SMC_SC4	OGLE004817.37–725536.5	0.556467	2450450.12401	19.09	19.97	20.11
SMC_SC4	OGLE004758.51–725430.6	0.618294	2450450.39021	19.25	19.93	20.45
SMC_SC4	OGLE004550.82–725342.1	0.612531	2450450.33796	19.08	19.65	20.06
SMC_SC4	OGLE004800.43–725222.7	0.518919	2450450.51520	19.23	19.86	20.27
SMC_SC4	OGLE004756.26–725217.6	0.592250	2450450.17243	19.09	19.70	20.14
SMC_SC4	OGLE004754.45–725212.1	0.586127	2450450.34334	19.10	20.02	20.11
SMC_SC4	OGLE004805.17–725144.4	0.509540	2450450.41483	19.24	19.61	20.04
SMC_SC4	OGLE004755.07–725141.5	0.504549	2450450.23360	18.96	19.42	19.73
SMC_SC4	OGLE004528.73–725109.7	0.656889	2450450.12283	19.09	19.70	–
SMC_SC4	OGLE004616.38–724926.7	0.648315	2450450.36557	19.14	19.78	20.31
SMC_SC4	OGLE004814.17–724837.4	0.536911	2450450.13189	19.30	19.91	20.27
SMC_SC4	OGLE004808.76–724351.2	0.618879	2450450.32033	19.02	19.62	20.13
SMC_SC4	OGLE004742.57–724315.5	0.552044	2450450.11251	19.32	19.91	20.21
SMC_SC4	OGLE004816.18–724249.1	0.642870	2450450.50173	18.85	19.57	19.84
SMC_SC4	OGLE004620.66–724246.6	0.596697	2450450.44950	18.86	19.42	–
SMC_SC4	OGLE004615.10–724135.5	0.647222	2450450.36154	19.19	19.77	20.32
SMC_SC4	OGLE004651.47–724040.8	0.649493	2450450.63333	18.92	19.51	19.87
SMC_SC4	OGLE004532.76–724018.2	0.579954	2450450.00568	19.06	19.60	20.00
SMC_SC4	OGLE004758.16–723929.7	0.549696	2450450.49921	19.04	19.60	–
SMC_SC4	OGLE004621.06–723918.3	0.570390	2450450.54191	19.30	19.85	–
SMC_SC4	OGLE004703.95–723915.8	0.554071	2450450.30318	18.99	19.49	–
SMC_SC5	OGLE005135.39–733417.0	0.559560	2450450.27158	19.36	20.00	–
SMC_SC5	OGLE005112.92–733302.6	0.586115	2450450.38079	18.43	19.04	19.41
SMC_SC5	OGLE005040.93–733245.8	0.687076	2450450.24528	18.71	19.30	19.66
SMC_SC5	OGLE005019.77–733131.4	0.511557	2450450.37167	18.58	19.29	19.80
SMC_SC5	OGLE004827.91–733108.7	0.637818	2450450.37974	19.04	19.62	20.01
SMC_SC5	OGLE004852.08–733034.5	0.563893	2450450.24775	19.26	19.77	20.27
SMC_SC5	OGLE005045.05–732738.8	0.570909	2450450.04667	18.97	19.41	19.71
SMC_SC5	OGLE005026.32–732418.2	0.422681	2450450.12730	19.59	20.11	20.23
SMC_SC5	OGLE004924.05–732231.3	0.585875	2450450.18674	19.73	20.58	21.24
SMC_SC5	OGLE005009.50–732105.8	0.599056	2450450.03930	19.26	20.01	20.59
SMC_SC5	OGLE005042.77–732103.0	0.656440	2450450.61300	19.03	19.67	20.13
SMC_SC5	OGLE005049.36–731917.6	0.630189	2450450.21295	19.35	20.05	20.57

Table 2

Continued

Field	Star ID	$P$ [days]	$T_0$ [HJD]	$I$ [mag]	$V$ [mag]	$B$ [mag]
SMC_SC5	OGLE004833.02-731800.0	0.535611	2450450.10067	19.38	19.97	20.36
SMC_SC5	OGLE005019.26-731610.0	0.608400	2450450.29679	19.24	19.88	20.31
SMC_SC5	OGLE004924.31-731447.2	0.545795	2450450.36610	19.49	20.14	20.65
SMC_SC5	OGLE004828.10-731442.2	0.586267	2450450.58290	18.78	19.28	—
SMC_SC5	OGLE005025.83-731403.0	0.599855	2450450.28478	19.45	20.17	—
SMC_SC5	OGLE005024.07-731349.0	0.566477	2450450.33383	19.06	19.59	20.00
SMC_SC5	OGLE004835.73-731330.1	0.584920	2450450.35112	19.25	19.84	20.28
SMC_SC5	OGLE004922.63-731220.9	0.578897	2450450.00291	19.06	19.87	—
SMC_SC5	OGLE005120.92-730920.1	0.549932	2450450.27920	19.28	19.96	20.30
SMC_SC5	OGLE004940.50-730901.2	0.596414	2450450.11857	19.50	20.43	20.95
SMC_SC5	OGLE004838.59-730820.1	0.648218	2450450.47363	18.84	19.61	19.93
SMC_SC5	OGLE005110.48-730750.0	0.431720	2450450.09690	19.61	20.13	20.25
SMC_SC5	OGLE004913.17-730651.0	0.620062	2450450.19862	19.22	19.91	20.30
SMC_SC5	OGLE004951.17-730620.3	0.624850	2450450.48463	19.12	19.86	20.06
SMC_SC5	OGLE004907.44-730617.5	0.625806	2450450.03943	19.57	20.48	21.06
SMC_SC5	OGLE004845.03-730445.3	0.569002	2450450.49550	19.81	20.72	21.27
SMC_SC5	OGLE004954.79-730321.3	0.803567	2450450.43899	19.01	19.66	20.03
SMC_SC5	OGLE004859.12-730226.6	0.564530	2450450.16304	19.34	—	19.97
SMC_SC5	OGLE004859.75-730111.2	0.636837	2450450.26670	19.60	20.43	20.99
SMC_SC5	OGLE004906.31-725930.6	0.643771	2450450.14844	19.05	19.68	20.07
SMC_SC5	OGLE004903.38-725750.1	0.606646	2450450.58766	19.14	19.97	20.05
SMC_SC5	OGLE004854.14-725710.6	0.603874	2450450.25172	19.09	19.59	20.03
SMC_SC5	OGLE004938.26-725616.5	0.516923	2450450.50677	19.55	20.16	—
SMC_SC5	OGLE005001.12-725402.6	0.619444	2450450.27737	19.42	20.15	20.61
SMC_SC5	OGLE004936.31-725229.2	0.642318	2450450.43365	19.10	19.72	20.08
SMC_SC5	OGLE005126.54-725205.3	0.543700	2450450.26863	19.21	19.83	20.20
SMC_SC5	OGLE004935.53-725113.9	0.634333	2450450.46663	19.11	19.80	20.21
SMC_SC5	OGLE005015.78-725020.6	0.684064	2450450.33727	18.81	19.34	19.77
SMC_SC5	OGLE004841.02-724731.3	0.517022	2450450.01453	19.25	19.81	20.22
SMC_SC5	OGLE004907.86-724443.6	0.627245	2450450.18015	19.33	19.92	20.34
SMC_SC5	OGLE004955.56-724200.4	0.662868	2450450.47838	18.88	19.49	19.91
SMC_SC6	OGLE005314.86-732622.7	0.591032	2450450.36230	19.11		
SMC_SC6	OGLE005427.69-732534.0	0.592581	2450450.09052	19.02	19.64	20.17
SMC_SC6	OGLE005415.18-732401.2	0.568968	2450450.15960	19.08	19.68	20.13
SMC_SC6	OGLE005146.64-732350.2	0.589878	2450450.27402	19.17	19.70	20.22
SMC_SC6	OGLE005147.81-732338.6	0.643648	2450450.04518	19.00	19.62	20.10
SMC_SC6	OGLE005412.35-732244.3	0.562833	2450450.39412	19.01	19.49	19.78
SMC_SC6	OGLE005216.92-732104.6	0.602526	2450450.04994	19.16	19.77	20.16
SMC_SC6	OGLE005253.73-731858.8	0.635921	2450450.34560	18.92	19.46	19.80
SMC_SC6	OGLE005142.15-731719.9	0.612405	2450450.50647	18.89	19.33	19.64
SMC_SC6	OGLE005342.12-731642.7	0.575976	2450450.21173	19.09	19.64	20.00
SMC_SC6	OGLE005308.68-731542.2	0.685501	2450450.45818	18.90	19.53	19.92
SMC_SC6	OGLE005244.35-731258.6	0.570412	2450450.52856	19.48	20.11	20.31
SMC_SC6	OGLE005415.82-731137.2	0.688832	2450450.57601	18.99	19.68	19.98
SMC_SC6	OGLE005408.31-730948.2	0.543769	2450450.03629	19.29	19.61	20.39
SMC_SC6	OGLE005312.51-730832.5	0.532397	2450450.12466	19.25	19.84	19.97
SMC_SC6	OGLE005311.88-730832.4	0.600040	2450450.12622	19.06	19.42	19.97
SMC_SC6	OGLE005253.76-730523.5	0.501068	2450450.46047	19.50	20.11	20.29
SMC_SC6	OGLE005251.40-730430.7	0.511478	2450450.17757	19.50	20.04	20.36
SMC_SC6	OGLE005326.07-730414.0	0.683569	2450450.26657	19.01	19.64	20.09
SMC_SC6	OGLE005144.52-730150.8	0.524808	2450450.12880	19.36	19.89	20.25
SMC_SC6	OGLE005302.56-730133.3	0.598191	2450450.42114	19.25	19.75	20.24
SMC_SC6	OGLE005249.73-730053.2	0.513645	2450450.42402	19.36	19.82	20.10
SMC_SC6	OGLE005318.13-725759.4	0.616994	2450450.34480	19.02	19.60	19.85
SMC_SC6	OGLE005202.85-725707.3	0.798955	2450450.50349	19.13	20.13	20.52
SMC_SC6	OGLE005424.14-725310.0	0.584825	2450450.18230	19.24	19.91	20.34
SMC_SC6	OGLE005126.54-725205.3	0.543707	2450450.24597	19.33	19.69	—
SMC_SC6	OGLE005300.26-725136.6	0.403584	2450450.19951	19.50	20.01	20.36
SMC_SC6	OGLE005415.50-725039.2	0.530955	2450450.48345	19.10	19.65	20.35
SMC_SC6	OGLE005428.43-724840.3	0.579410	2450450.24757	19.11	19.71	20.22
SMC_SC6	OGLE005417.74-724755.1	0.611398	2450450.48150	19.16	20.00	20.50
SMC_SC6	OGLE005243.99-724740.5	0.611447	2450450.20140	19.02	19.53	19.84
SMC_SC6	OGLE005211.81-724646.2	0.544049	2450450.41321	19.22	19.71	20.06
SMC_SC6	OGLE005202.38-724638.8	0.757914	2450450.45342	19.11	19.84	20.34
SMC_SC6	OGLE005358.43-724538.9	0.553928	2450450.00327	19.30	19.82	—
SMC_SC6	OGLE005139.52-724334.0	0.475422	2450450.04202	19.48	19.88	20.63
SMC_SC6	OGLE005300.78-724245.7	0.567517	2450450.35721	19.33	20.10	20.67
SMC_SC6	OGLE005200.56-724209.9	0.587970	2450450.03713	19.44	20.09	20.56

Table 2

Continued

Field	Star ID	$P$ [days]	$T_0$ [HJD]	$I$ [mag]	$V$ [mag]	$B$ [mag]
SMC_SC6	OGLE005142.52–724101.0	0.645529	2450450.10923	18.98	20.02	20.13
SMC_SC6	OGLE005229.18–723902.5	0.612973	2450450.46846	19.50	20.15	20.68
SMC_SC6	OGLE005410.32–723725.7	0.628749	2450450.56958	18.48	19.02	19.10
SMC_SC6	OGLE005329.90–723600.3	0.612264	2450450.33708	19.07	—	—
SMC_SC6	OGLE005236.85–723519.5	0.510831	2450450.13267	18.73	—	—
SMC_SC6	OGLE005334.07–723508.1	0.637590	2450450.49360	18.81	19.36	19.78
SMC_SC6	OGLE005324.12–723308.1	0.627479	2450450.52660	19.02	—	—
SMC_SC6	OGLE005348.57–723239.5	0.683095	2450450.38499	19.04	19.68	20.08
SMC_SC7	OGLE005450.07–732054.3	0.525835	2450450.23858	19.37	19.93	20.31
SMC_SC7	OGLE005515.21–731918.2	0.589480	2450450.15940	18.74	19.25	19.61
SMC_SC7	OGLE005721.02–731838.7	0.577696	2450450.45161	19.16	19.71	20.06
SMC_SC7	OGLE005632.59–731833.6	0.554398	2450450.27031	19.39	19.96	20.38
SMC_SC7	OGLE005613.46–731820.3	0.497593	2450450.19533	19.27	19.80	20.21
SMC_SC7	OGLE005640.54–731620.5	0.629896	2450450.45481	19.09	19.64	20.04
SMC_SC7	OGLE005441.17–731436.4	0.573377	2450450.27215	19.18	—	—
SMC_SC7	OGLE005505.47–731251.9	0.615814	2450450.44364	19.02	19.60	19.98
SMC_SC7	OGLE005612.31–731222.5	0.619898	2450450.14896	19.16	19.71	20.09
SMC_SC7	OGLE005723.57–731136.1	0.562479	2450450.28445	19.03	19.83	20.11
SMC_SC7	OGLE005504.67–731106.4	0.463068	2450450.00221	19.35	19.82	20.09
SMC_SC7	OGLE005614.52–731023.8	0.701793	2450450.42131	19.15	19.91	20.10
SMC_SC7	OGLE005616.96–730901.6	0.615658	2450450.13501	18.94	19.35	19.45
SMC_SC7	OGLE005658.96–730850.0	0.641613	2450450.52869	18.68	19.21	19.73
SMC_SC7	OGLE005656.87–730850.2	0.545403	2450450.00371	19.17	19.73	20.00
SMC_SC7	OGLE005711.65–730825.3	0.503516	2450450.43009	19.20	20.05	19.95
SMC_SC7	OGLE005451.81–730710.6	0.568647	2450450.19817	19.12	19.67	19.96
SMC_SC7	OGLE005503.04–730548.6	0.483923	2450450.16703	19.51	20.04	20.46
SMC_SC7	OGLE005538.66–730529.9	0.549977	2450450.28564	19.31	19.82	20.24
SMC_SC7	OGLE005720.63–730416.8	0.535267	2450450.18999	19.08	19.63	19.85
SMC_SC7	OGLE005451.94–730359.6	0.502497	2450450.41120	19.45	19.87	20.34
SMC_SC7	OGLE005519.19–730344.7	0.532526	2450450.42787	18.94	19.42	19.66
SMC_SC7	OGLE005609.42–730323.2	0.521781	2450450.35807	19.29	19.82	—
SMC_SC7	OGLE005701.66–730321.8	0.562350	2450450.50541	19.39	19.98	20.51
SMC_SC7	OGLE005606.56–730242.1	0.617223	2450450.54979	18.81	19.37	19.81
SMC_SC7	OGLE005439.11–730215.5	0.467226	2450450.28134	19.26	19.70	19.95
SMC_SC7	OGLE005723.39–730159.6	0.631765	2450450.41415	19.19	19.79	20.26
SMC_SC7	OGLE005709.44–725959.9	0.651567	2450450.58377	19.29	19.88	20.31
SMC_SC7	OGLE005656.16–725859.3	0.560855	2450450.52527	19.11	19.72	19.99
SMC_SC7	OGLE005701.41–725857.4	0.597714	2450450.50969	19.19	19.97	20.60
SMC_SC7	OGLE005518.27–725722.5	0.601763	2450450.20072	19.08	19.66	20.00
SMC_SC7	OGLE005543.38–725605.7	0.570396	2450450.23060	19.17	19.79	20.09
SMC_SC7	OGLE005719.62–725540.7	0.433862	2450450.00829	19.51	20.03	20.24
SMC_SC7	OGLE005609.38–725516.2	0.550922	2450450.49719	19.22	19.77	20.16
SMC_SC7	OGLE005534.90–725455.5	0.525181	2450450.00933	19.43	19.96	20.32
SMC_SC7	OGLE005725.77–725438.5	0.605840	2450450.46988	19.23	19.84	20.23
SMC_SC7	OGLE005549.04–725335.1	0.629768	2450450.43985	18.97	19.54	20.49
SMC_SC7	OGLE005629.88–725213.0	0.422334	2450450.34766	18.25	19.07	—
SMC_SC7	OGLE005642.92–725121.3	0.596850	2450450.58695	19.32	19.91	20.18
SMC_SC7	OGLE005610.54–725044.6	0.619313	2450450.03600	18.97	19.62	—
SMC_SC7	OGLE005519.94–725036.5	0.584305	2450450.36965	19.08	19.68	20.07
SMC_SC7	OGLE005458.09–724948.9	0.447471	2450450.40267	19.35	19.74	20.14
SMC_SC7	OGLE005530.88–724846.8	0.719676	2450450.34261	19.04	19.59	19.99
SMC_SC7	OGLE005428.43–724840.3	0.579403	2450450.28475	19.16	19.70	—
SMC_SC7	OGLE005701.81–724743.5	0.584233	2450450.57791	19.16	19.82	20.22
SMC_SC7	OGLE005641.27–724723.7	0.492409	2450450.19256	19.69	20.24	20.82
SMC_SC7	OGLE005705.34–724623.5	0.622923	2450450.54472	19.16	19.89	20.40
SMC_SC7	OGLE005509.14–724607.5	0.616585	2450450.25617	19.10	19.68	20.12
SMC_SC7	OGLE005559.00–724508.1	0.649027	2450450.19604	18.92	19.45	—
SMC_SC7	OGLE005522.80–724505.4	0.606779	2450450.25089	19.01	19.63	20.05
SMC_SC7	OGLE005714.69–724355.5	0.659379	2450450.50109	19.02	19.69	20.17
SMC_SC7	OGLE005728.64–724135.0	0.602738	2450450.28085	19.03	19.67	20.87
SMC_SC7	OGLE005506.01–723610.0	0.605221	2450450.44714	19.20	19.85	20.16
SMC_SC7	OGLE005719.60–723529.9	0.642422	2450450.12457	19.54	20.31	20.77
SMC_SC7	OGLE005649.36–723506.8	0.560811	2450450.27144	19.28	20.16	19.68
SMC_SC7	OGLE005728.85–723454.6	0.416260	2450450.25103	19.72	20.35	20.62
SMC_SC7	OGLE005646.16–723452.2	0.445986	2450450.24824	19.51	20.05	20.44
SMC_SC7	OGLE005536.64–723410.8	0.519047	2450450.34160	19.43	20.05	20.53
SMC_SC7	OGLE005440.61–723349.7	0.623934	2450450.33909	19.34	20.12	20.48
SMC_SC7	OGLE005643.06–722650.5	0.631589	2450450.35773	19.27	20.01	20.40

Table 2

Continued

Field	Star ID	$P$ [days]	$T_0$ [HJD]	$I$ [mag]	$V$ [mag]	$B$ [mag]
SMC_SC7	OGLE005450.02-722645.0	0.607395	2450450.49414	19.35	19.96	20.29
SMC_SC7	OGLE005714.48-722620.0	0.672639	2450450.15216	18.99	19.74	20.15
SMC_SC8	OGLE005957.83-730647.6	0.447303	2450450.22832	19.44	19.92	20.26
SMC_SC8	OGLE005838.13-730642.1	0.627792	2450450.30504	19.17	19.80	—
SMC_SC8	OGLE005741.65-730440.5	0.524742	2450450.27770	19.14	19.64	—
SMC_SC8	OGLE005723.39-730159.6	0.631767	2450450.35540	19.22	19.79	—
SMC_SC8	OGLE005836.07-730053.0	0.630980	2450450.26619	19.10	19.79	20.04
SMC_SC8	OGLE005835.93-730031.2	0.574874	2450450.48963	19.14	19.59	19.86
SMC_SC8	OGLE005857.37-725948.2	0.620118	2450450.60867	19.04	19.55	20.51
SMC_SC8	OGLE005858.64-725935.2	0.602382	2450450.15569	19.17	19.70	—
SMC_SC8	OGLE005740.55-725726.1	0.624170	2450450.11934	19.23	19.72	20.18
SMC_SC8	OGLE005848.70-725713.4	0.595096	2450450.36930	18.97	19.50	19.91
SMC_SC8	OGLE005813.16-725530.0	0.587750	2450450.23033	18.87	19.34	19.68
SMC_SC8	OGLE005725.77-725438.5	0.605842	2450450.47481	19.26	19.89	—
SMC_SC8	OGLE010010.82-725400.0	0.619525	2450450.60344	18.54	19.12	19.40
SMC_SC8	OGLE005832.99-725355.4	0.618296	2450450.54077	19.30	19.95	20.66
SMC_SC8	OGLE005849.63-724943.2	0.6111491	2450450.10523	18.96	19.50	19.95
SMC_SC8	OGLE005928.02-724852.2	0.649107	2450450.16574	19.36	20.05	—
SMC_SC8	OGLE005915.72-724831.7	0.552687	2450450.32443	19.23	19.85	20.12
SMC_SC8	OGLE005849.95-724547.3	0.621396	2450450.60899	18.77	19.32	19.65
SMC_SC8	OGLE005744.12-724324.8	0.609748	2450450.32304	19.18	19.80	20.17
SMC_SC8	OGLE005752.70-724306.1	0.594998	2450450.33809	19.07	19.67	20.17
SMC_SC8	OGLE005849.59-724211.6	0.654940	2450450.07426	19.06	19.72	20.14
SMC_SC8	OGLE005728.64-724135.0	0.602733	2450450.28289	19.08	19.71	—
SMC_SC8	OGLE005943.17-724047.4	0.466507	2450450.10486	19.46	19.97	20.61
SMC_SC8	OGLE005752.74-723901.8	0.557047	2450450.07982	19.27	19.87	20.34
SMC_SC8	OGLE005820.37-723841.4	0.640661	2450450.63266	18.76	19.36	19.87
SMC_SC8	OGLE005737.26-723819.1	0.687028	2450450.41877	19.20	19.84	20.31
SMC_SC8	OGLE005806.86-723811.7	0.614224	2450450.35984	18.89	19.48	19.89
SMC_SC8	OGLE005933.82-723607.1	0.592689	2450450.27611	19.13	19.76	20.08
SMC_SC8	OGLE005803.73-723602.0	0.625510	2450450.27711	19.21	19.89	20.44
SMC_SC8	OGLE005728.85-723454.6	0.416258	2450450.25297	19.76	20.29	20.55
SMC_SC8	OGLE005905.67-723050.1	0.564275	2450450.29164	19.21	19.77	20.17
SMC_SC8	OGLE005926.80-722526.1	0.655476	2450450.53693	19.04	19.84	—
SMC_SC8	OGLE005912.21-722210.0	0.618612	2450450.24236	18.61	19.20	19.53
SMC_SC8	OGLE005740.36-721934.4	0.587544	2450450.06503	19.17	20.09	19.84
SMC_SC8	OGLE005923.37-721908.0	0.581425	2450450.31135	19.05	—	20.19
SMC_SC8	OGLE010003.88-721705.3	0.626031	2450450.27826	19.20	19.96	20.31
SMC_SC8	OGLE005939.69-721545.8	0.645881	2450450.59242	19.06	19.69	20.08
SMC_SC8	OGLE005942.61-721452.8	0.563973	2450450.49746	19.04	19.56	20.01
SMC_SC9	OGLE010302.96-725901.7	0.603724	2450450.40897	19.12	19.72	20.02
SMC_SC9	OGLE010121.94-725637.1	0.547720	2450450.39358	19.12	19.62	20.05
SMC_SC9	OGLE010140.83-725606.1	0.481324	2450450.23152	19.45	19.98	—
SMC_SC9	OGLE010134.33-725427.4	0.433496	2450450.27980	19.40	19.94	20.17
SMC_SC9	OGLE010247.17-725227.1	0.621718	2450450.14189	19.13	19.68	20.06
SMC_SC9	OGLE010301.04-725208.8	0.693484	2450450.48943	19.18	19.83	20.24
SMC_SC9	OGLE010110.58-725042.6	0.646732	2450450.38567	19.09	19.69	20.06
SMC_SC9	OGLE010202.86-725034.1	0.593268	2450450.22450	19.23	19.76	20.91
SMC_SC9	OGLE010046.71-724839.8	0.561071	2450450.17836	18.99	19.54	20.03
SMC_SC9	OGLE010135.31-724803.7	0.558498	2450450.45648	19.13	19.65	20.08
SMC_SC9	OGLE010244.66-724613.8	0.542216	2450450.42714	19.10	19.64	20.16
SMC_SC9	OGLE010147.55-724554.7	0.717976	2450450.46503	18.45	18.97	19.26
SMC_SC9	OGLE010144.36-724332.6	0.634869	2450450.38200	19.04	19.60	19.86
SMC_SC9	OGLE010218.16-724304.7	0.580739	2450450.39420	19.04	19.60	19.98
SMC_SC9	OGLE010130.04-724210.6	0.590646	2450450.38560	19.40	19.91	20.20
SMC_SC9	OGLE010249.81-724157.9	0.620329	2450450.32296	19.01	19.61	19.95
SMC_SC9	OGLE010124.81-724157.0	0.533424	2450450.43280	19.36	19.90	20.24
SMC_SC9	OGLE010219.99-724143.4	0.512806	2450450.30438	19.04	19.53	19.64
SMC_SC9	OGLE010245.87-724107.0	0.567842	2450450.00285	19.17	19.73	20.17
SMC_SC9	OGLE010249.16-723736.4	0.708618	2450450.43466	19.14	19.79	20.29
SMC_SC9	OGLE010232.98-723534.4	0.557708	2450450.44018	19.17	19.67	20.06
SMC_SC9	OGLE010042.76-723415.3	0.535404	2450450.12583	19.48	20.04	—
SMC_SC9	OGLE010148.87-723212.1	0.754425	2450450.60292	18.88	19.25	19.52
SMC_SC9	OGLE010102.42-722844.1	0.657289	2450450.38268	19.16	19.80	20.37
SMC_SC9	OGLE010127.68-722700.0	0.630669	2450450.50706	19.33	20.06	20.38
SMC_SC9	OGLE010235.05-722255.4	0.603652	2450450.32844	19.37	19.96	20.32
SMC_SC9	OGLE010302.01-722213.0	0.514681	2450450.01568	19.27	19.91	20.09
SMC_SC9	OGLE010125.15-721904.9	0.654753	2450450.25568	18.85	19.47	19.84
SMC_SC9	OGLE010255.53-721643.6	0.593289	2450450.38856	18.82	19.33	19.74

Table 2

Concluded

Field	Star ID	$P$ [days]	$T_0$ [HJD]	$I$ [mag]	$V$ [mag]	$B$ [mag]
SMC_SC9	OGLE010326.63–721409.8	0.559307	2450450.32551	19.34	20.00	–
SMC_SC9	OGLE010052.12–721051.7	0.583265	2450450.43190	18.99	19.52	19.91
SMC_SC9	OGLE010045.01–720946.8	0.576859	2450450.07281	18.86	19.38	19.66
SMC_SC9	OGLE010324.09–720545.7	0.637207	2450450.04729	19.26	19.92	20.27
SMC_SC10	OGLE010455.18–725156.2	0.541616	2450450.39115	19.30	20.05	20.25
SMC_SC10	OGLE010503.64–725130.2	0.636944	2450450.39096	18.96	19.60	20.02
SMC_SC10	OGLE010343.94–725126.3	0.633037	2450450.10653	19.05	19.57	20.04
SMC_SC10	OGLE010432.13–724958.4	0.629954	2450450.47432	18.74	19.14	–
SMC_SC10	OGLE010338.67–724949.6	0.556086	2450450.47132	18.90	19.23	19.61
SMC_SC10	OGLE010448.82–724945.3	0.650334	2450450.12730	19.06	19.69	20.13
SMC_SC10	OGLE010501.92–724932.8	0.496103	2450450.36959	19.21	19.78	–
SMC_SC10	OGLE010450.99–724700.3	0.488994	2450450.31966	19.25	19.80	20.26
SMC_SC10	OGLE010442.62–724627.5	0.614622	2450450.44923	19.15	19.76	20.10
SMC_SC10	OGLE010409.82–724611.9	0.644261	2450450.55242	19.03	19.59	19.80
SMC_SC10	OGLE010553.86–724436.4	0.598127	2450450.47656	19.04	19.61	20.05
SMC_SC10	OGLE010446.17–724232.1	0.573893	2450450.54631	19.14	19.68	20.22
SMC_SC10	OGLE010338.90–724034.3	0.648203	2450450.63146	19.35	19.87	20.18
SMC_SC10	OGLE010452.90–724025.9	0.433623	2450450.21677	19.19	19.57	19.90
SMC_SC10	OGLE010523.13–723829.2	0.535858	2450450.09156	19.57	20.17	–
SMC_SC10	OGLE010403.41–723557.5	0.584941	2450450.47549	19.30	19.86	–
SMC_SC10	OGLE010446.99–723456.8	0.503731	2450450.32942	19.27	19.86	20.25
SMC_SC10	OGLE010448.37–722912.1	0.578879	2450450.03632	19.34	19.91	20.23
SMC_SC10	OGLE010515.10–722528.3	0.551041	2450450.27579	19.09	19.67	19.90
SMC_SC10	OGLE010516.55–722526.5	0.455958	2450450.22964	19.50	20.09	20.52
SMC_SC10	OGLE010415.01–722458.5	0.654505	2450450.59721	18.82	19.38	19.81
SMC_SC10	OGLE010427.09–722320.1	0.560479	2450450.13678	19.25	19.80	20.20
SMC_SC10	OGLE010431.15–722125.8	0.533258	2450450.23179	19.22	19.73	20.11
SMC_SC10	OGLE010434.89–721722.2	0.578845	2450450.45562	19.40	20.09	20.40
SMC_SC10	OGLE010326.63–721409.8	0.559307	2450450.32346	19.36	19.94	–
SMC_SC10	OGLE010445.62–721035.2	0.681351	2450450.22679	18.99	19.63	20.03
SMC_SC10	OGLE010332.65–720944.8	0.614248	2450450.23793	18.74	19.14	19.43
SMC_SC10	OGLE010535.93–720621.6	0.453841	2450450.09247	19.50	19.93	20.34
SMC_SC10	OGLE010446.97–720620.4	0.749592	2450450.50803	19.05	19.68	20.12
SMC_SC10	OGLE010324.09–720545.7	0.637209	2450450.05105	19.25	19.89	–
SMC_SC10	OGLE010603.11–720500.6	0.568160	2450450.21802	19.41	20.04	20.27
SMC_SC10	OGLE010344.20–720407.9	0.632913	2450450.26553	19.00	19.54	19.87
SMC_SC10	OGLE010455.87–720320.2	0.643898	2450450.51066	18.92	19.51	19.88
SMC_SC10	OGLE010509.23–720218.0	0.599654	2450450.26605	18.94	19.55	19.90
SMC_SC10	OGLE010411.34–720152.0	0.573859	2450450.01135	19.56	20.18	20.65
SMC_SC10	OGLE010611.31–715732.7	0.643145	2450450.26498	19.00	19.64	20.04
SMC_SC10	OGLE010403.48–715721.6	0.616891	2450450.33076	19.30	19.91	20.38
SMC_SC10	OGLE010359.90–715720.0	0.611870	2450450.30397	18.62	19.16	19.50
SMC_SC11	OGLE010800.59–730739.5	0.623917	2450450.28937	19.06	–	–
SMC_SC11	OGLE010847.54–730521.1	0.568063	2450450.34059	19.33	19.94	–
SMC_SC11	OGLE010842.27–730411.2	0.755208	2450450.44509	19.00	19.60	20.06
SMC_SC11	OGLE010834.94–730005.6	0.557271	2450450.11485	19.10	19.67	–
SMC_SC11	OGLE010725.95–725941.5	0.580738	2450450.30387	18.93	19.58	19.76
SMC_SC11	OGLE010823.35–725813.9	0.785200	2450450.32256	18.78	19.46	19.98
SMC_SC11	OGLE010640.65–725637.3	0.574302	2450450.04248	19.15	19.69	–
SMC_SC11	OGLE010627.06–725434.5	0.649536	2450450.53118	18.69	19.30	–
SMC_SC11	OGLE010653.16–725406.9	0.562441	2450450.03668	19.14	19.63	–
SMC_SC11	OGLE010836.97–725321.6	0.619422	2450450.22081	19.16	19.76	–
SMC_SC11	OGLE010909.88–724646.4	0.658584	2450450.35160	18.99	19.60	–
SMC_SC11	OGLE010909.66–724149.8	0.565590	2450450.21404	18.95	19.54	19.85
SMC_SC11	OGLE010654.39–724145.5	0.578431	2450450.50201	19.18	19.71	20.04
SMC_SC11	OGLE010648.19–723553.4	0.525160	2450450.22892	19.34	19.94	20.21
SMC_SC11	OGLE010633.08–723544.9	0.627022	2450450.39759	19.32	19.99	20.45
SMC_SC11	OGLE010804.44–723349.3	0.646477	2450450.33238	18.88	19.54	19.91
SMC_SC11	OGLE010846.41–723243.2	0.579876	2450450.01153	19.13	19.73	20.18
SMC_SC11	OGLE010728.57–723052.9	0.575224	2450450.54781	19.00	19.58	19.84
SMC_SC11	OGLE010838.76–722758.0	0.622726	2450450.53749	18.87	19.32	19.58
SMC_SC11	OGLE010655.60–722754.5	0.510401	2450450.05283	19.12	19.55	19.85
SMC_SC11	OGLE010742.39–722352.8	0.529878	2450450.08817	18.89	19.43	19.71
SMC_SC11	OGLE010848.72–722342.9	0.626908	2450450.36074	19.14	19.71	20.00
SMC_SC11	OGLE010818.39–722315.5	0.561962	2450450.46985	19.23	19.71	–
SMC_SC11	OGLE010721.87–721825.9	0.672973	2450450.37001	18.99	19.62	19.84
SMC_SC11	OGLE010802.60–721600.8	0.629378	2450450.55957	18.84	19.43	19.82
SMC_SC11	OGLE010734.49–721429.8	0.646715	2450450.38464	18.98	19.60	20.00
SMC_SC11	OGLE010838.27–721333.3	0.578293	2450450.36868	19.11	19.68	20.05

Table 3

c-type RR Lyrae stars from the SMC

Field	Star ID	$P$ [days]	$T_0$ [HJD]	$I$ [mag]	$V$ [mag]	$B$ [mag]
SMC_SC1	OGLE003908.31–735426.8	0.281006	2450450.20606	18.99	19.32	–
SMC_SC1	OGLE003744.55–734750.5	0.368667	2450450.23920	19.15	19.61	19.83
SMC_SC1	OGLE003737.93–734706.2	0.352683	2450450.33501	19.32	19.77	20.04
SMC_SC1	OGLE003853.80–732328.0	0.345051	2450450.27801	19.38	19.83	20.15
SMC_SC1	OGLE003706.77–730551.2	0.293459	2450450.06673	19.20	19.43	19.64
SMC_SC2	OGLE003946.61–733332.6	0.309804	2450450.17994	19.42	19.85	20.44
SMC_SC2	OGLE004007.32–731338.8	0.343159	2450450.22418	19.44	19.94	20.27
SMC_SC2	OGLE003934.35–730433.9	0.351432	2450450.11490	19.10	19.56	–
SMC_SC3	OGLE004330.74–733416.0	0.320723	2450450.20162	19.29	19.72	19.94
SMC_SC3	OGLE004444.50–732833.1	0.370527	2450450.20609	19.06	19.79	20.63
SMC_SC3	OGLE004245.08–730939.7	0.311416	2450450.18060	19.27	19.64	19.85
SMC_SC3	OGLE004322.30–725905.5	0.346199	2450450.27457	19.13	19.56	19.82
SMC_SC3	OGLE004327.25–724542.4	0.344124	2450450.23623	19.20	19.70	19.92
SMC_SC4	OGLE004808.56–731003.6	0.326195	2450450.07486	19.28	19.75	20.04
SMC_SC4	OGLE004624.67–730050.3	0.357261	2450450.08049	18.93	19.57	20.13
SMC_SC4	OGLE004744.89–725530.1	0.297777	2450450.00931	19.18	19.51	19.79
SMC_SC4	OGLE004633.73–725253.8	0.302182	2450450.19175	19.50	19.93	20.21
SMC_SC4	OGLE004631.02–724658.8	0.308220	2450450.28206	19.24	19.63	19.86
SMC_SC5	OGLE004848.01–732714.6	0.345412	2450450.27837	19.11	19.41	19.64
SMC_SC5	OGLE004845.41–730826.4	0.372181	2450450.15355	19.36	19.87	20.31
SMC_SC5	OGLE005115.64–724739.2	0.280936	2450450.18512	19.16	19.82	19.82
SMC_SC5	OGLE004902.13–724513.6	0.310884	2450450.24968	19.18	19.69	20.17
SMC_SC5	OGLE004840.40–724402.4	0.354180	2450450.16695	19.32	19.79	–
SMC_SC6	OGLE005155.37–724909.5	0.363936	2450450.06872	19.39	19.93	20.15
SMC_SC7	OGLE005556.74–732133.6	0.349140	2450450.24051	19.38	–	–
SMC_SC7	OGLE005503.23–731907.8	0.313536	2450450.24977	19.27	19.62	19.86
SMC_SC7	OGLE005609.24–731504.8	0.277551	2450450.17346	18.78	19.31	19.65
SMC_SC7	OGLE005601.69–730338.5	0.427773	2450450.20740	18.79	19.30	19.70
SMC_SC7	OGLE005621.27–730046.9	0.351118	2450450.18641	19.24	19.71	19.92
SMC_SC7	OGLE005633.68–725700.0	0.441252	2450450.25788	19.11	19.65	–
SMC_SC7	OGLE005618.62–725209.7	0.370889	2450450.14595	18.92	19.36	19.64
SMC_SC7	OGLE005725.22–724432.7	0.337364	2450450.27667	18.88	19.53	19.95
SMC_SC7	OGLE005527.97–724136.8	0.371404	2450450.00957	19.22	19.75	20.03
SMC_SC7	OGLE005601.43–724026.2	0.283717	2450450.16025	19.58	–	–
SMC_SC7	OGLE005451.72–723850.4	0.277966	2450450.00890	19.03	19.31	–
SMC_SC8	OGLE010029.57–725454.2	0.343212	2450450.33141	19.41	19.92	20.21
SMC_SC8	OGLE005853.75–725335.2	0.371910	2450450.09010	19.26	19.75	20.13
SMC_SC8	OGLE005913.99–724719.4	0.313798	2450450.30113	19.44	19.89	20.24
SMC_SC8	OGLE005754.46–723248.2	0.283746	2450450.13031	18.52	19.29	20.11
SMC_SC8	OGLE005913.24–722418.6	0.378142	2450450.07666	19.33	19.77	20.37
SMC_SC9	OGLE010151.77–730020.1	0.385044	2450450.04714	19.37	–	–
SMC_SC9	OGLE010029.57–725454.2	0.343216	2450450.32098	19.47	19.91	–
SMC_SC9	OGLE010246.69–725030.1	0.262593	2450450.01799	18.80	19.09	19.42
SMC_SC9	OGLE010316.37–724816.2	0.370538	2450450.13873	19.34	19.83	19.79
SMC_SC9	OGLE010220.67–723753.6	0.261244	2450450.16592	19.61	19.95	–
SMC_SC9	OGLE010256.60–723431.0	0.445955	2450450.03397	19.03	19.56	19.91
SMC_SC9	OGLE010232.82–723147.1	0.347329	2450450.25602	19.11	19.58	19.71
SMC_SC9	OGLE010231.17–722134.0	0.346288	2450450.20236	19.25	19.73	20.04
SMC_SC9	OGLE010148.62–721836.8	0.368215	2450450.00787	19.22	19.66	19.95
SMC_SC9	OGLE010245.99–721132.7	0.294040	2450450.16386	19.32	19.73	19.92
SMC_SC9	OGLE010249.92–720947.1	0.316409	2450450.14857	19.38	19.82	20.10
SMC_SC10	OGLE010316.37–724816.2	0.370556	2450450.12805	19.42	–	–
SMC_SC10	OGLE010349.04–724400.1	0.369181	2450450.10959	19.22	19.72	20.09
SMC_SC10	OGLE010453.59–723756.0	0.339862	2450450.14489	19.27	19.75	20.12
SMC_SC11	OGLE010647.29–723053.7	0.362757	2450450.22340	19.25	19.73	20.07
SMC_SC11	OGLE010850.08–723030.3	0.355358	2450450.19533	19.20	19.72	19.89
SMC_SC11	OGLE010731.44–721745.7	0.345769	2450450.19988	19.41	19.89	20.20
SMC_SC11	OGLE010718.63–721723.0	0.358960	2450450.24852	19.25	19.75	20.10

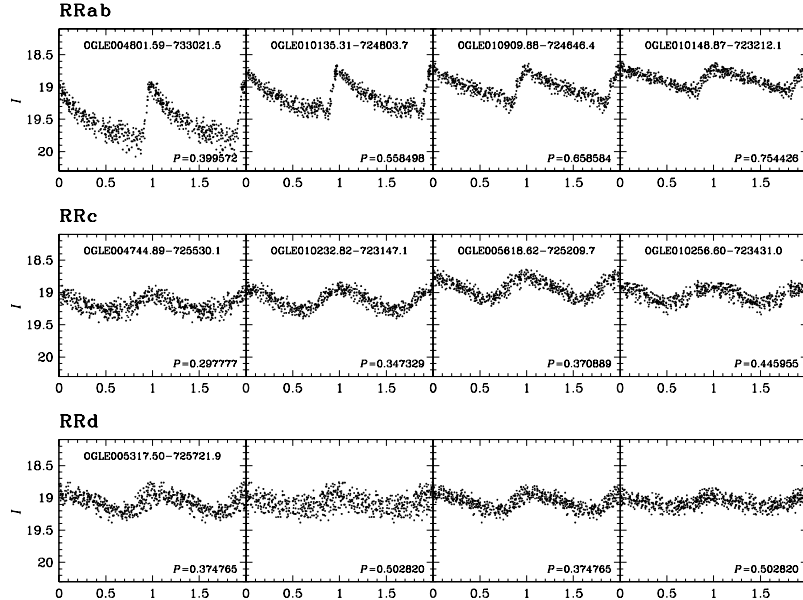


Fig. 2. Exemplary light curves of RR Lyr stars from the SMC. In the top row light curves of four typical RRab stars arranged according to the periods are presented. In the middle row a sample of four RRc stars is presented. Bottom row shows the light curves of an exemplary RRD variable – original photometric data folded with the shorter and longer periods, and light curves of each mode after subtraction of the other period variability.

## 6.2 Double-Mode RR Lyr Stars

RRd stars discovered in the SMC are listed in Table 4. 59 such objects were detected but 57 of them are unique. Two stars are located in the overlapping regions between fields and they were discovered independently. Table 4 lists the field name, star ID, period of the first overtone, period of the fundamental mode, period ratio, and finally *IVB* intensity-mean magnitudes. Other parameters, individual *BVI* measurements and finding charts are available from the OGLE INTERNET archive.

## 6.3 Other Stars

Table 5 presents a list of 19 detected short-period variables and a few other variable stars. The table contains 20 entries because one object was identified twice in the overlapping region of fields SMC\_SC5 and SMC\_SC6. Consecutive columns of Table 5 represent the same data as in Tables 2 and 3. Most stars from the list are probably  $\delta$  Sct stars. Two stars: OGLE005542.36-732105.3 and OGLE010118.99-723323.8, are double-mode pulsators, with the period ratios 0.76259 and 0.77098, respectively. In Table 5 we present longer periods of both stars.

Table 4  
d-type RR Lyrae stars from the SMC

Field	Star ID	$P_1$ [days]	$P_0$ [days]	$P_1/P_0$	$I$ [mag]	$V$ [mag]	$B$ [mag]
SMC_SC1	OGLE003638.62–734034.2	0.361795	0.485969	0.744482	18.94	19.41	19.66
SMC_SC1	OGLE003659.06–733452.1	0.372989	0.500389	0.745398	19.05	19.50	19.76
SMC_SC1	OGLE003703.18–733216.6	0.394705	0.529477	0.745462	19.13	19.64	20.01
SMC_SC1	OGLE003803.07–732829.2	0.380053	0.509537	0.745879	19.22	19.73	20.04
SMC_SC1	OGLE003619.43–732553.0	0.419186	0.561512	0.746531	18.97	19.55	–
SMC_SC1	OGLE003838.05–731453.7	0.410901	0.550465	0.746462	18.94	19.53	19.83
SMC_SC1	OGLE003901.05–730751.1	0.397228	0.532444	0.746047	19.22	19.82	–
SMC_SC1	OGLE003733.92–730607.7	0.364203	0.489339	0.744275	19.23	19.71	20.02
SMC_SC2	OGLE004228.21–734532.0	0.424805	0.569703	0.745661	18.94	–	–
SMC_SC2	OGLE004105.53–734149.6	0.387770	0.520756	0.744629	19.07	19.54	19.85
SMC_SC2	OGLE004222.96–733223.8	0.364102	0.488706	0.745034	19.29	19.82	20.13
SMC_SC2	OGLE004203.77–732544.8	0.378924	0.508841	0.744680	19.36	19.84	20.28
SMC_SC2	OGLE004126.10–731644.9	0.379489	0.509092	0.745422	19.33	19.92	20.25
SMC_SC2	OGLE004214.47–731644.6	0.379294	0.508928	0.745281	18.95	19.45	19.74
SMC_SC2	OGLE004051.20–731417.8	0.375345	0.503322	0.745736	19.09	19.64	19.90
SMC_SC2	OGLE004004.29–730044.3	0.367739	0.493854	0.744632	19.30	19.82	20.09
SMC_SC2	OGLE004038.76–730023.5	0.367415	0.493166	0.745012	19.39	20.00	20.41
SMC_SC3	OGLE004222.96–733223.8	0.364102	0.488706	0.745034	19.30	19.86	–
SMC_SC3	OGLE004253.47–732750.6	0.354895	0.476748	0.744408	19.14	19.53	19.75
SMC_SC3	OGLE004348.60–732434.9	0.390466	0.523846	0.745382	19.17	19.60	19.94
SMC_SC3	OGLE004335.78–732058.5	0.423200	0.566785	0.746667	18.89	19.36	19.68
SMC_SC3	OGLE004358.07–730157.7	0.362730	0.486752	0.745204	19.20	19.58	19.83
SMC_SC3	OGLE004251.11–724804.4	0.379104	0.508353	0.745750	19.18	19.67	19.95
SMC_SC3	OGLE004230.85–724651.0	0.370284	0.496839	0.745281	19.05	19.45	–
SMC_SC4	OGLE004615.67–731940.4	0.360343	0.483994	0.744520	19.34	19.90	20.36
SMC_SC4	OGLE004745.68–731516.2	0.402812	0.540698	0.744985	19.20	19.75	20.11
SMC_SC4	OGLE004817.90–723921.2	0.395636	0.530727	0.745461	19.12	19.65	–
SMC_SC5	OGLE004949.44–731703.1	0.426080	0.571101	0.746068	19.17	19.64	19.85
SMC_SC5	OGLE005017.68–730910.6	0.382452	0.513099	0.745378	19.14	19.58	19.93
SMC_SC5	OGLE005118.41–730502.2	0.435088	0.582519	0.746907	18.83	19.32	19.62
SMC_SC5	OGLE005049.46–730030.1	0.373855	0.501734	0.745127	19.13	19.72	19.96
SMC_SC5	OGLE005023.79–724047.7	0.364916	0.490275	0.744309	19.33	19.79	–
SMC_SC6	OGLE005342.24–732514.1	0.363768	0.488306	0.744959	19.34	19.84	20.21
SMC_SC6	OGLE005155.91–732428.5	0.378633	0.508443	0.744692	19.16	19.81	19.94
SMC_SC6	OGLE005152.03–730348.6	0.407388	0.545692	0.746553	19.22	19.72	19.97
SMC_SC6	OGLE005317.50–725721.9	0.374765	0.502820	0.745327	19.07	19.63	19.92
SMC_SC6	OGLE005401.42–724728.7	0.378620	0.507628	0.745862	19.34	19.99	20.36
SMC_SC6	OGLE005237.14–724651.2	0.372969	0.500557	0.745107	19.61	20.01	19.69
SMC_SC6	OGLE005430.51–724240.9	0.366688	0.492198	0.745002	18.99	19.48	19.75
SMC_SC6	OGLE005346.56–723637.1	0.388001	0.519872	0.746339	19.14	19.61	19.89
SMC_SC7	OGLE005449.66–724259.5	0.427425	0.573399	0.745423	18.94	19.45	19.84
SMC_SC7	OGLE005628.74–724247.9	0.392275	0.525936	0.745862	19.05	–	–
SMC_SC7	OGLE005430.51–724240.9	0.366691	0.492209	0.744990	19.00	19.46	–
SMC_SC7	OGLE005453.68–724150.7	0.392306	0.526163	0.745595	19.12	19.64	20.01
SMC_SC7	OGLE005724.34–724031.3	0.396128	0.531318	0.745558	19.16	19.81	20.27
SMC_SC8	OGLE005948.83–730107.6	0.382381	0.512899	0.745529	19.34	19.88	20.18
SMC_SC8	OGLE0010016.23–724726.9	0.369094	0.495560	0.744802	19.25	19.75	19.99
SMC_SC8	OGLE005906.43–722145.3	0.367714	0.493503	0.745109	19.32	19.87	20.27
SMC_SC9	OGLE010233.77–724728.8	0.366232	0.491380	0.745314	19.18	19.66	–
SMC_SC9	OGLE010038.72–724455.6	0.370112	0.496828	0.744950	19.20	19.63	19.89
SMC_SC9	OGLE010212.03–724109.6	0.374545	0.502773	0.744958	19.16	19.66	–
SMC_SC9	OGLE010301.09–722910.9	0.364565	0.489423	0.744888	19.41	19.86	19.98
SMC_SC9	OGLE010102.15–721554.4	0.365668	0.491466	0.744035	19.14	19.61	19.83
SMC_SC10	OGLE010558.62–723119.0	0.364133	0.488757	0.745018	18.86	19.24	19.55
SMC_SC10	OGLE010334.17–722141.0	0.376754	0.505382	0.745484	19.16	19.70	19.93
SMC_SC11	OGLE010902.50–725018.9	0.371349	0.498079	0.745562	19.42	19.93	–
SMC_SC11	OGLE010728.50–724527.6	0.366752	0.492110	0.745264	19.53	20.05	20.42
SMC_SC11	OGLE010632.81–722035.0	0.359977	0.483701	0.744214	19.29	19.79	20.11
SMC_SC11	OGLE010721.27–721939.9	0.370842	0.498288	0.744232	19.38	19.90	20.28

T a b l e 5  
Other variable stars from the SMC

Field	Star ID	$P$ [days]	$T_0$ [HJD]	$I$ [mag]	$V$ [mag]	$B$ [mag]
SMC_SC2	OGLE004157.65–730119.9	0.203325	2450450.06205	19.26	19.82	20.26
SMC_SC2	OGLE004115.08–725407.8	0.251083	2450450.23158	19.44	19.78	–
SMC_SC4	OGLE004616.17–731416.1	0.503192	2450450.06849	18.26	19.02	19.45
SMC_SC5	OGLE005008.48–725916.5	0.252511	2450450.12714	18.86	19.49	19.86
SMC_SC5	OGLE005135.18–724438.1	0.238996	2450450.05630	19.07	19.69	–
SMC_SC6	OGLE005424.16–730529.4	0.211744	2450450.09308	18.94	19.44	19.79
SMC_SC6	OGLE005259.56–725605.3	0.356721	2450450.18734	18.27	19.28	19.69
SMC_SC6	OGLE005353.94–725207.7	0.193607	2450450.08955	19.23	19.71	21.18
SMC_SC6	OGLE005145.04–724446.5	0.232651	2450450.16994	19.12	19.67	20.15
SMC_SC6	OGLE005135.18–724438.1	0.238996	2450450.08302	19.11	19.66	20.22
SMC_SC7	OGLE005542.36–732105.3	0.341130	2450450.04449	18.88	19.37	19.75
SMC_SC7	OGLE005456.26–730814.3	0.237242	2450450.06554	18.95	19.51	19.74
SMC_SC7	OGLE005507.46–724434.0	0.570419	2450450.40706	18.38	18.75	–
SMC_SC7	OGLE005653.43–724340.6	0.227619	2450450.00403	18.49	–	–
SMC_SC7	OGLE005521.33–723751.8	0.357436	2450450.12745	18.50	19.01	19.47
SMC_SC7	OGLE005558.04–722633.2	0.252600	2450450.17328	19.18	–	20.28
SMC_SC8	OGLE005848.58–724941.6	0.234350	2450450.21723	18.99	19.44	19.77
SMC_SC8	OGLE005739.23–724449.5	0.161751	2450450.01635	19.33	19.83	20.30
SMC_SC8	OGLE005740.47–721413.1	0.226250	2450450.16643	18.93	19.39	19.77
SMC_SC9	OGLE010118.99–723323.8	0.279555	2450450.02007	19.09	19.64	19.98

## 7. Basic Parameters of RR Lyr Stars

### 7.1 Period Distribution

Distribution of periods of RR Lyr stars is an indicator of the morphology of the horizontal branch of the population of old, metal-weak stars. The final period search was carried out with program TATRY by Schwarzenberg-Czerny (2002, private communication). The program works in two steps. First, it calculates a periodogram and identifies its peaks. Then the corresponding peak frequencies are examined in detail to find the best one and its corresponding ephemeris. TATRY provides also reliable estimation of period errors, what we could check comparing periods of stars located in the overlapping regions of the adjacent fields. Accuracy of periods for the vast majority of the RR Lyr stars is better than  $10^{-5}$  days. The period errors for each star are included in the OGLE INTERNET archive data.

Period distribution for the global sample is shown in Fig. 3. The mean period of ab-type RR Lyr stars, and simultaneously the most preferred period, is  $\langle P_{ab} \rangle = 0.589$  days. This result is in the ideal agreement with Graham's (1975) determination of the mean period of RRab variables near NGC121.  $\langle P_{ab} \rangle$  is believed to be an indicator of the mean metallicity – it increases with decreas-

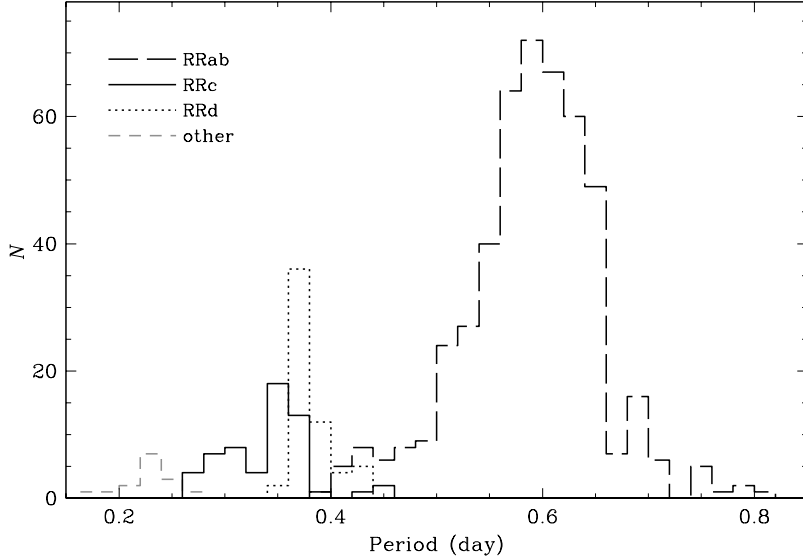


Fig. 3. Distribution of periods for RR Lyr stars from the SMC. The bins are 0.02 days wide. Long-dashed line represents period distribution of RRab stars, solid line – RRc stars, dotted line – RRD stars (first overtone periods), and short-dashed – other stars.

ing metallicity. However, one should remember that Clement *et al.* (2001), in a study of the properties of the RR Lyr stars in Galactic globular clusters, suggested that the correlation breaks down when the mean period is larger than 0.60 days.

The period distribution of the first overtone pulsators indicates two preferred periods. Most of the RRc stars prefer periods near  $\langle P_c \rangle = 0.357$  days, but there is also a significant excess of stars around  $P = 0.29$  days. Such short-period RR Lyr stars also exist in other environments, *e.g.*, in the LMC (Alcock *et al.* 1996) and in the globular cluster IC 4499 (Walker and Nemec 1996). It has been suggested (van Albada and Baker 1973) that these stars are second overtone (RRe) pulsators. The pulsation of RR Lyr stars in overtone modes was theoretically analyzed by Stellingwerf *et al.* (1987).

RRd variable stars (first-overtone periods) and RRc stars occupy different, but overlapping regions in the period distribution histogram. Periods of the first overtone in the double-mode RR Lyr stars range from about 0.354 to 0.435 days with the mean period  $\langle P_d \rangle = 0.382$  days. Single-mode first-overtone pulsators have typically shorter or longer periods than double-mode RR Lyr stars (we found three candidates for RRc stars with periods between 0.428 and 0.446 days).

## 7.2 Intensity Mean Photometry

BVI intensity mean photometry of each object from our sample of RR Lyr

Table 6

Cross-identification of stars detected in the overlapping regions

Star ID	Fields
OGLE004227.44–733655.1	SMC_SC2 SMC_SC3
OGLE004222.96–733223.8	SMC_SC2 SMC_SC3
OGLE004225.29–730349.8	SMC_SC2 SMC_SC3
OGLE004533.91–733240.2	SMC_SC3 SMC_SC4
OGLE004526.76–732801.7	SMC_SC3 SMC_SC4
OGLE004531.73–732634.2	SMC_SC3 SMC_SC4
OGLE004533.00–731255.1	SMC_SC3 SMC_SC4
OGLE004533.33–730120.2	SMC_SC3 SMC_SC4
OGLE004528.73–725109.7	SMC_SC3 SMC_SC4
OGLE004827.91–733108.7	SMC_SC4 SMC_SC5
OGLE004828.10–731442.2	SMC_SC4 SMC_SC5
OGLE004833.02–731800.0	SMC_SC4 SMC_SC5
OGLE004835.73–731330.1	SMC_SC4 SMC_SC5
OGLE005126.54–725205.3	SMC_SC5 SMC_SC6
OGLE005135.18–724438.1	SMC_SC5 SMC_SC6
OGLE005428.43–724840.3	SMC_SC6 SMC_SC7
OGLE005430.51–724240.9	SMC_SC6 SMC_SC7
OGLE005723.39–730159.6	SMC_SC7 SMC_SC8
OGLE005725.77–725438.5	SMC_SC7 SMC_SC8
OGLE005728.63–724135.0	SMC_SC7 SMC_SC8
OGLE005728.85–723454.6	SMC_SC7 SMC_SC8
OGLE010029.58–725454.3	SMC_SC8 SMC_SC9
OGLE010316.37–724816.2	SMC_SC8 SMC_SC9
OGLE010326.63–721409.8	SMC_SC9 SMC_SC10
OGLE010324.09–720545.7	SMC_SC9 SMC_SC10

candidates was derived by integrating the light curve converted to intensity units. The light curve was approximated by the Fourier series of fifth order and results were converted back to the magnitude scale. Accuracy of the mean *I*-band photometry is about 0.02 mag while that of the *V*-band and *B*-band about 0.03 mag and 0.08 mag, respectively, what is a consequence of smaller number of observations in the *BV*-band filters.

To obtain the mean brightness of the SMC RR Lyr stars, we prepared histograms of the *BVI*-band apparent magnitudes separately for RRab, RRc and RRd variable stars. In the next step we fitted a Gaussian to each histogram, and obtained the most preferred brightness of these stars. Then we repeated this procedure using magnitudes corrected for interstellar extinction. Results are presented in Tables 7 and 8.

T a b l e 7  
Mean  $I$ ,  $V$  and  $B$  magnitudes of RR Lyr stars

Type	$I$	$\sigma_I$	$V$	$\sigma_V$	$B$	$\sigma_B$
RRab	$19.14 \pm 0.01$	0.20	$19.74 \pm 0.01$	0.23	$20.10 \pm 0.01$	0.25
RRc	$19.27 \pm 0.01$	0.15	$19.73 \pm 0.01$	0.15	$20.00 \pm 0.01$	0.23
RRd	$19.17 \pm 0.01$	0.17	$19.69 \pm 0.01$	0.20	$19.94 \pm 0.02$	0.22

T a b l e 8  
Mean  $I$ ,  $V$  and  $B$  extinction free magnitudes of RR Lyr stars

Type	$I_0$	$\sigma_{I_0}$	$V_0$	$\sigma_{V_0}$	$B_0$	$\sigma_{B_0}$
RRab	$18.97 \pm 0.01$	0.20	$19.45 \pm 0.01$	0.23	$19.73 \pm 0.01$	0.25
RRc	$19.10 \pm 0.01$	0.15	$19.45 \pm 0.01$	0.15	$19.63 \pm 0.02$	0.24
RRd	$19.00 \pm 0.01$	0.17	$19.42 \pm 0.01$	0.20	$19.58 \pm 0.02$	0.24

### 7.3 Period-Amplitude Relation for RR Lyr Stars

We determined amplitudes of light curves by fitting Fourier series of fifth order and calculating difference between minimal and maximal values of the function. The period-amplitude diagram for the SMC RR Lyr stars is shown in Fig. 4. The symbols are as follows: black dots indicate the position of RRab and RRc stars, triangles and diamonds represent RRd stars (first-overtone and fundamental mode, respectively) and crosses mark other stars.

Well-known dependence of the amplitudes on periods for RRab stars is seen, although some stars, especially RRab with shorter periods, do not follow this relation. The first overtone RR Lyr variables show weak correlation of amplitudes and periods but, inversely to the fundamental mode pulsators, amplitude slightly increases with increasing periods.

Comparison of amplitudes of fundamental mode and first overtone of RRd stars confirms that the dominant mode of pulsation in the majority of double-mode RR Lyr stars is the first overtone. The mean ratio of the first-harmonic and fundamental mode amplitudes is about 1.6.

### 7.4 Fourier Parameters of Light Curve Decomposition

Fourier decomposition of light curves of RR Lyr stars has been widely used for analyzing their properties. Several empirical and theoretical relations between Fourier parameters and the physical parameters of RR Lyr variables have been proposed (*e.g.*, Kovács and Walker 2001).

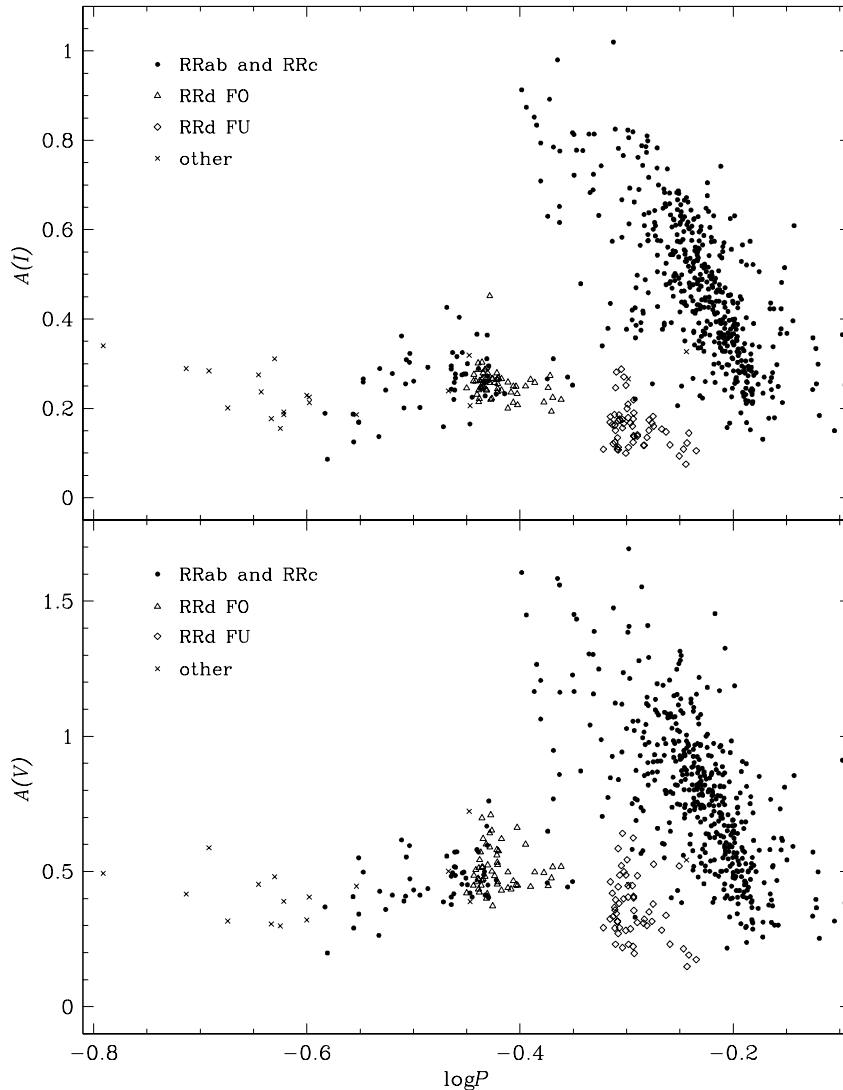


Fig. 4. Period– $I$ -amplitude (upper panel) and period– $V$ -amplitude (lower panel) diagrams for RR Lyr stars from the SMC. Small dots represent RRab and RRc stars, triangles and diamonds represent RRd stars (first-overtone and fundamental mode, respectively), and crosses mark other stars.

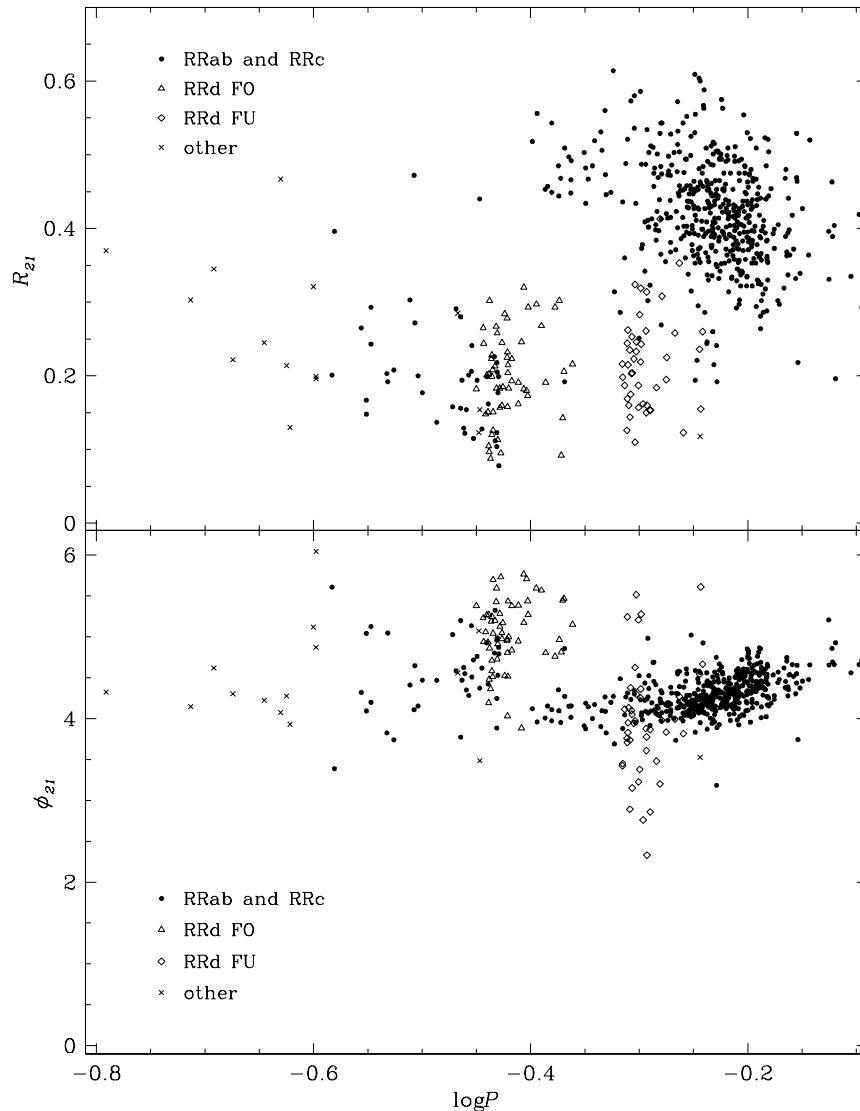


Fig. 5.  $R_{21}$  and  $\phi_{21}$  vs.  $\log P$  diagrams for RR Lyr stars from the SMC. Small dots represent RRab and RRc stars, triangles and diamonds represent RRd stars (first-overtone and fundamental mode, respectively), and crosses mark other stars.

Fifth order Fourier series were fitted to the magnitude scale  $I$ -band light curve. Then, we derived  $R_{21}$ ,  $R_{31}$ ,  $\phi_{21}$  and  $\phi_{31}$  Fourier parameters, where  $R_{ij} = A_i/A_j$ ,  $\phi_{ij} = \phi_i - i\phi_j$ .  $A_i$  and  $\phi_i$  are the amplitudes and phases of  $(i-1)$  harmonic of the Fourier decomposition of light curve.

Light curves of double-mode pulsators were decomposed to the sum of two Fourier series of fourth order corresponding to both periodicities. Then we calculated Fourier parameters for both pulsating modes.

In Fig. 5 we present  $R_{21} - \log P$  and  $\phi_{21} - \log P$  diagrams constructed for our sample of RR Lyr stars. The first-overtone and fundamental mode pulsators are well separated in both diagrams.  $R_{21}$  for RRab stars tends to become smaller as the periods become longer, what means that the light curves of long-period ab-type RR Lyr are more sinusoidal than the light curves of short-period RRab stars.

Fourier parameters of the first-overtone mode of RRd stars fall in the sequence of the single-mode first overtone RR Lyr stars, but the fundamental mode pulsation have  $R_{21}$  smaller than corresponding single-mode RR Lyr variables. This means that fundamental-mode pulsations in RRd stars have not only smaller amplitude, but the light curves are more sinusoidal than the light curves of RRab stars.

## 7.5 Petersen Diagram

RR Lyr stars pulsating simultaneously in the fundamental mode and the first overtone are especially interesting as a test of structural and evolutionary models of the horizontal branch stars. A powerful tool for diagnosing stellar models and for determination of masses, absolute magnitudes and metallicities of stars is the so called Petersen diagram, in which the period ratio of two excited modes is plotted against the longer period. Position of stars in the Peterson diagram can be precisely determined, because periods are the observables that are measured with the highest precision.

In Fig. 6 we present Petersen diagram of all discovered RRd stars. For comparison, we also plotted in the same diagram double mode RR Lyr stars from the LMC (catalog of RR Lyr stars from the LMC will be published in the forthcoming paper).

The SMC and LMC double-mode RR Lyr stars evidently form the same relation  $P_1/P_0$  vs.  $P_0$ , but RRd stars from the SMC prefer longer periods and larger period ratios than the LMC RRd stars. Pulsation models suggest that the position of a given RRd star in the Petersen diagram is a function of stellar mass and metallicity. We can expect that the shift in the Petersen diagram between RRd stars from the LMC and the SMC is caused by different mean metallicity of RR Lyr stars in both galaxies. More information about analysis of the Peterson diagrams can be found in Popiel'ski, Dziembowski and Cassisi (2000).

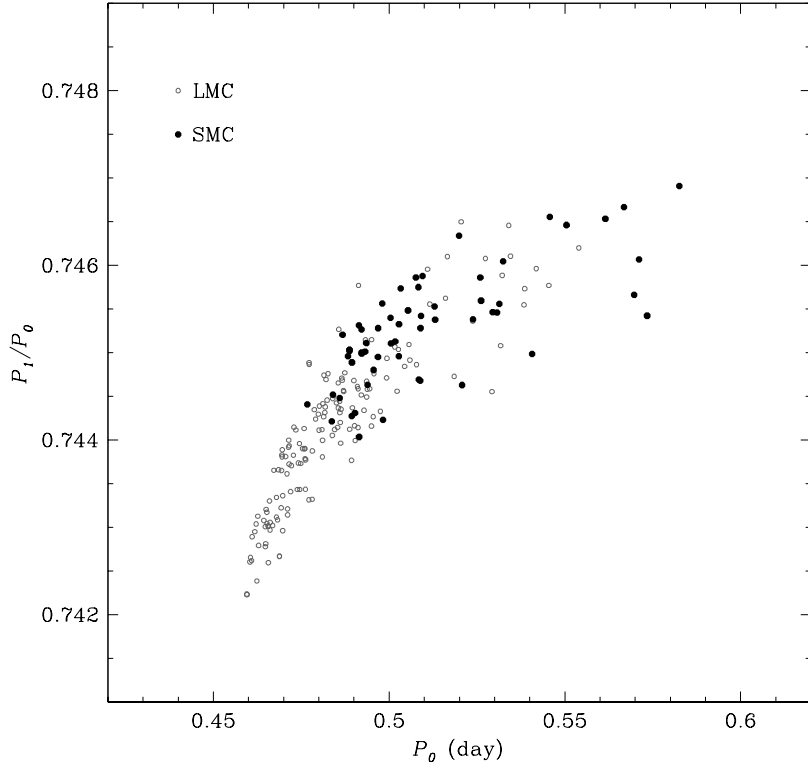


Fig. 6. Petersen diagram for the LMC and SMC double-mode RR Lyr stars. The open circles mark RRd stars from the LMC, the filled circles represent RRd stars from the SMC.

## 8. Completeness of the Catalog

We estimated completeness of the Catalog of RR Lyr stars in similar manner as for the catalog of Cepheids from the Small Magellanic Cloud (Udalski *et al.* 1999), *i.e.*, by comparison of objects located in the overlapping regions of the adjacent fields. Ten such regions exist between our fields (Fig. 1) allowing to perform 20 tests of paring objects from a given and neighboring fields. In total, 57 stars from Tables 2–5 should be theoretically paired with counterparts in the overlapping fields. We found counterparts in 50 cases. Counterparts of four from seven unpaired objects had the number of observations smaller than 50 and thus they were not searched for variability. Smaller number of measurement points in the edge regions of the fields is due to non-perfect pointing of the telescope. The remaining three objects were missed because of severe blending with another stars or because of unusually small amplitude of variability.

Udalski *et al.* (1998a) estimated completeness of detection of stars in the SMC OGLE fields using artificial star tests. For stars as bright as RR Lyr the completeness was found to be between 90 and 95%, depending on the field density. In our sample completeness should be much higher, because the stars

are being detected on the DIA reference images, obtained by co-adding 20 best frames for each field. We conclude that the completeness of our sample should be about 90%.

## 9. Conclusions

The long term photometric surveys of dense stellar systems may provide large samples of all types of variable stars (Paczyński 2000). In this paper we present the catalog of RR Lyr variable stars – objects playing a major role in studies of the processes of stellar pulsation, post-main-sequence evolution of stars, calibration of extragalactic distances, and structure and age of galaxies. This is the largest sample of RR Lyr variables detected in the SMC so far.

We reported detection of 57 double-mode RR Lyr stars. We also found RR Lyr variables exhibiting two closely spaced frequencies, most probably related to non-radial pulsations.

About 10% of the detected RR Lyr variables are RRc stars. Next 10% of the whole sample are RRd variables. Relatively small number of the first-overtone

T a b l e 9  
RR Lyr stars close to the SMC clusters

Field	Star ID	Cluster name OGLE-CL-	Alternative cluster name	Cluster radius [""]	Distance from the center [""]
SMC_SC2	OGLE004222.96–733223.8	SMC0014		24	33
SMC_SC3	OGLE004504.31–725623.9	SMC0024		57	68
SMC_SC4	OGLE004526.76–732801.7	SMC0027	B39	36	51
SMC_SC4	OGLE004610.66–730355.6	SMC0183		10	1
SMC_SC4	OGLE004817.88–731815.2	SMC0048	B47	49	67
SMC_SC5	OGLE004833.02–731800.0	SMC0048	B47	49	25
SMC_SC5	OGLE004907.44–730617.5	SMC0052	H86-104	18	25
SMC_SC5	OGLE004913.17–730651.0	SMC0052	H86-104	18	21
SMC_SC5	OGLE004922.63–731220.9	SMC0053		30	30
SMC_SC5	OGLE004924.05–732231.3	SMC0054	L39	27	30
SMC_SC5	OGLE004924.31–731447.2	SMC0195	BS42	28	35
SMC_SC5	OGLE004954.79–730321.3	SMC0057	B52	49	67
SMC_SC5	OGLE004936.31–725229.2	SMC0058	H86-109	36	51
SMC_SC5	OGLE005120.92–730920.1	SMC0069	NGC290	36	36
SMC_SC6	OGLE005202.85–725707.3	SMC0074	K29,L44	42	44
SMC_SC6	OGLE005243.99–724740.5	SMC0085	B66	25	17
SMC_SC7	OGLE005549.04–725335.1	SMC0105	H86-165	44	54
SMC_SC7	OGLE005612.31–731222.5	SMC0106		26	15
SMC_SC8	OGLE005820.37–723841.4	SMC0113	L61-331	24	19
SMC_SC11	OGLE010728.50–724527.6	SMC0156	L80	41	42
SMC_SC11	OGLE010836.97–725321.6	SMC0159	NGC419	102	80

pulsators and the value of the average period of RRab stars (0.589 days) places the SMC RR Lyr stars near the Oosterhoff type I group.

Additionally, we conducted a search of RR Lyr stars in the SMC clusters. Discovery of RR Lyr variables in the clusters younger than NGC121 (hosting four RR Lyr stars), would have a significant consequences on our understanding of evolution of old, solar-mass stars. We used the OGLE catalog of the SMC clusters (Pietrzyński *et al.* 1998) containing 238 clusters, their coordinates and angular sizes. We scanned our sample of RR Lyr variables looking for stars in a distance smaller than 1.5 cluster radius from the cluster center. We obtained the list of 21 RR Lyr stars located close to the line-of-sight to, in total, 19 SMC clusters. Only in two cases (OGLE-CL-SMC0048 and OGLE-CL-SMC0052) we detected two RR Lyr stars in the cluster neighborhood. It is very probable that the majority of these cases are just optical coincidences, because more or less similar number of stars could be expected in the background of SMC clusters (comparing the area of the clusters to the area of all our fields). Nevertheless, because of potential importance of the discovery of RR Lyr variables in the SMC clusters, we provide in Table 9 the list of stars located close to the SMC clusters.

**Acknowledgements.** We would like to thank Prof. Bohdan Paczyński for many discussions and valuable suggestions. We are very grateful to Prof. Wojciech Dzembrowski for helping us in the classification of stars. The paper was partly supported by the Polish KBN grant BST to Warsaw University Observatory. Partial support for the OGLE project was provided with the NSF grants AST-9820314 and AST-0204908 and NASA grant NAG5-12212 to B. Paczyński. We acknowledge usage of the Digitized Sky Survey which was produced at the Space Telescope Science Institute based on photographic data obtained using the UK Schmidt Telescope, operated by the Royal Observatory Edinburgh.

## REFERENCES

- Alard, C., and Lupton, R.H. 1998, *Astrophys. J.*, **503**, 325.  
 Alard, C. 2000, *Astron. Astrophys. Suppl. Ser.*, **144**, 363.  
 Alcock, C., *et al.* (MACHO team) 1993, *Nature*, **365**, 621.  
 Alcock, C., *et al.* (MACHO team) 1996, *Astron. J.*, **111**, 1146.  
 Aubourg, E., *et al.* (EROS team) 1993, *Nature*, **365**, 623.  
 Baade, W. 1952, *Trans. IAU*, **8**, 397.  
 Bono, G., Caputo, F., Castellani, V., and Marconi, M. 1997, *Astron. Astrophys. Suppl. Ser.*, **121**, 327.  
 Clement, C., *et al.* 2001, *Astron. J.*, **122**, 2587.  
 Dzembrowski, W., and Cassisi, S. 1999, *Acta Astron.*, **49**, 371.  
 Graham, J.A. 1975, *P.A.S.P.*, **87**, 641.  
 Kovács, G., *et al.* 2000, in: *IAU Colloq. 176*, “The Impact of Large-Scale Surveys on Pulsating Star Research”, Ed. L. Szabados and D.W. Kurtz, *ASP Conference Series*, Vol. **203**, 313.  
 Kovács, G., and Walker, A.R. 2001, *Astron. Astrophys.*, **371**, 579.  
 Moskalik, P. 2000, in: *IAU Colloq. 176*, “The Impact of Large-Scale Surveys on Pulsating Star Research”, Ed. L. Szabados and D.W. Kurtz, *ASP Conference Series*, Vol. **203**, 135.  
 Olech, A., *et al.* 1999, *Astron. J.*, **118**, 442.

- Olszewski, E.W., Schommer, R.A., and Aaronson, M. 1987, *Astron. J.*, **93**, 565.
- Paczyński, B. 2000, *P.A.S.P.*, **112**, 1281.
- Pietrzyński, G., Udalski, A., Kubiak, M., Szymański, M., Woźniak, P., and Żebruń, K. 1998, *Acta Astron.*, **48**, 175.
- Popielski, B.L., Dziembowski, W.A., and Cassisi, S. 2000, *Acta Astron.*, **50**, 491.
- Roberts, D.H., Lehár, J., and Dreher, J.W. 1987, *Astron. J.*, **93**, 968.
- Schechter, P.L., Saha, K., and Mateo, M. 1993, *P.A.S.P.*, **105**, 1342.
- Schlegel, D.J., Finkbeiner, D.P., and Davis, M. 1998, *Astrophys. J.*, **500**, 525.
- Schwarzenberg-Czerny, A. 1989, *MNRAS*, **241**, 153.
- Sharpee, B., Stark, M., Pritzl, B., Smith, H., Silbermann, N., Wilhelm, R., and Walker, A. 2002, *Astron. J.*, **124**, 2341.
- Smith, H.A., Silbermann, N.A., Baird, S.R., and Graham, J.A. 1992, *Astron. J.*, **104**, 1430.
- Stellingwerf, R.F., Gauchy, A., and Dickens, R.J. 1987, *Astrophys. J.*, **313**, L75.
- Stryker, L.L., Da Costa, G.S., and Mould, J.R. 1985, *Astrophys. J.*, **298**, 544.
- Thackeray, A.D. 1951, *The Observatory*, **71**, 219.
- Udalski, A., Kubiak, M., and Szymański, M. 1997, *Acta Astron.*, **47**, 319.
- Udalski, A., Szymański, M., Kubiak, M., Pietrzyński, G., Woźniak, P., and Żebruń, K. 1998a, *Acta Astron.*, **48**, 147.
- Udalski, A., Soszyński, I., Szymański, M., Kubiak, M., Pietrzyński, G., Woźniak, P., and Żebruń, K. 1998b, *Acta Astron.*, **48**, 563.
- Udalski, A., Soszyński, I., Szymański, M., Kubiak, M., Pietrzyński, G., Woźniak, P., and Żebruń, K. 1999, *Acta Astron.*, **49**, 437.
- van Albada, T.S., and Baker, N.H. 1973, *Astrophys. J.*, **185**, 477.
- Walker, A. 1989, *P.A.S.P.*, **101**, 570.
- Walker, A.R., and Nemec J.M. 1986, *Astron. J.*, **112**, 2026.
- Woźniak, P. R. 2000, *Acta Astron.*, **50**, 421.
- Żebruń, K., Soszyński, I., and Woźniak, P.R. 2001, *Acta Astron.*, **51**, 303.
- Żebruń, K., Soszyński, I., Woźniak, P., Udalski, A., Kubiak, M., Szymański, M., Pietrzyński, G., Szewczyk, O., and Wyrzykowski, L. 2001, *Acta Astron.*, **51**, 317.